In presenting the dissertation as a partial fulfillment of the requirements for an advanced degree from the Georgia Institute of Technology, I agree that the Library of the Institute shall make it available for inspection and circulation in accordance with its regulations governing materials of this type. I agree that permission to copy from, or to publish from, this dissertation may be granted by the professor under whose direction it was written, or, in his absence, by the Dean of the Graduate Division when such copying or publication is solely for scholarly purposes and does not involve potential financial gain. It is understood that any copying from, or publication of, this dissertation which involves potential financial gain will not be allowed without written permission.

7/25/68

THE FORMATION AND DESTRUCTION OF EXCITED HYDROGEN ATOMS AT HIGH IMPACT VELOCITIES

A THESIS

Presented to

The Faculty of the Graduate Division

by

Joseph Lee Edwards

In Partial Fulfillment ,

of the Requirements for the Degree

Doctor of Philosophy

in the School of Physics

Georgia Institute of Technology

May, 1970

THE FORMATION AND DESTRUCTION OF EXCITED HYDROGEN ATOMS

AT HIGH IMPACT VELOCITIES

Approved:

Chairman

Date approved by Chairman: 5-28-70

ACKNOWLEDGMENTS

It is indeed a pleasure to express my appreciation to Dr. E. W. Thomas for his continual guidance and encouragement during the performance of this research. His interest extended far beyond the duties of thesis advisor, and I am grateful for his untiring assistance. The careful reading and valuable comments of Dr. D. W. Martin and Dr. J. W. Hooper were responsible for numerous improvements in this manuscript; I am grateful for this help. The beneficial influence of other members of the faculty of the School of Physics is also appreciated.

I would like to thank Mr. J. C. Ford and Mr. F. T. Richey for their assistance in the construction of portions of the equipment. I also wish to express my appreciation to Mr. J. D. Dameron, Mr. G. A. Bearce, and Mr. V. B. Reynolds of the Mechanical Services Branch of the Engineering Experiment Station for their interest and excellent workmanship in fabricating several important parts of the apparatus. Thanks are also due to Mr. O. B. Francis for writing the computer program for reducing and analyzing the data, and to the Rich Electronic Computer Center for the donation of computer time.

This work was supported in part by the Controlled Thermonuclear Research Program, Division of Research, U. S. Atomic Energy Commission. A traineeship from the National Aeronautics and Space Administration permitted three years of concentrated graduate study. For both of these sources of support, I express my appreciation.

Special thanks go to Mrs. Lydia Geeslin for her careful typing of the manuscript.

TABLE OF CONTENTS

TABLE OF CONTENTS (Continued)

TABLE OF CONTENTS (Concluded)

LIST OF TABLES

LIST OF ILLUSTRATIONS

LIST OF ILLUSTRATIONS (Concluded)

ABSTRACT

A study has been made of the charge transfer processes whereby fast, neutral atoms of hydrogen are formed in the 3s, 3p, and 3d excited states as a result of the impact of protons on targets of helium and of nitrogen. The procedure involved quantitative measurement of the Balmer alpha radiation emitted in spontaneous decay of the excited atoms. The fact that the 3s, 3p, and 3d states have substantially different lifetimes permitted the use of a time-of-flight technique to identify separately their contributions to the emission. It was necessary to assess the influence of processes whereby the excited atoms were collisionally destroyed before undergoing spontaneous radiative decay. Detailed measurements of the collisional formation and destruction processes are presented for targets of He and N_2 for impact energies from 75 to 400 keV. An assessment is also made of the effect on the measurements of other secondary processes: cascade contributions from more highly excited states and the formation of ground state neutral atoms of hydrogen in the beam with the subsequent excitation or ionization of these atoms. Comparisons are made with theoretical predictions and with other experimental measurements.

The cross section for capture into the 3s state is by far the largest of the three capture cross sections and is larger for a nitrogen target than for helium. Cross sections for capture into the 3p and 3d states are one to two orders of magnitude smaller, but the

fraction of the atoms formed in the p and d states is slightly larger in nitrogen than in helium. There is agreement with other measurements within experimental error. Calculations utilizing the Born approximation are available for a target of helium, and there is agreement with the predictions for capture into the 3s and 3d states. However, the calculation for the 3p state appears to overestimate the cross section by a factor of at least four.

The cross sections for collisional destruction of atoms in the 3s state are several orders of magnitude larger than for electron capture into this state, and the magnitudes of the measured values are in agreement with theoretical predictions.

CHAPTER I

INTRODUCTION

Techniques for observing collision processes among atomic particles have provided science with some of its most valuable tools for probing the structure of matter. A knowledge of atomic collision processes is of great importance in verifying laws of particle interaction, and the subject has evoked considerable interest during the last several decades.

With the development of quantum mechanics, it became possible, in principle, to make calculations for any atomic collision process. However, computational difficulties have prevented exact calculations in most cases. Calculations for a collision process require the wave functions of all the collision partners. Wave functions of sufficient accuracy for the precise prediction of collision phenomena are not yet known except for hydrogenic atoms and ions. Furthermore, the quantum mechanical description of the dynamics of a collision process requires a set of wave functions which is complete in the mathematical sense and leads in practice to an almost intractable, infinite set of equations. Because of these complexities, exact computations appear to be impossible at the present time.

Recourse must therefore be made to simplifying approximations. Unfortunately, the validity of such approximations is, in general, impossible to assess in advance. Only by comparison with experimental

measurements can their validity be evaluated. However, once a theoretical approach has been thus verified, it is sometimes possible to extend it with confidence to situations for which experimental verification is impossible.

Any description of events which occur on an atomic scale must, in general, be given in terms of probabilities. This fact is due to an inherent property of nature and applies to all types of atomic collision processes. The concept of a collision cross section is frequently used to describe the probability of forming a particular post-collision system, and a mathematical development is given in Appendix I. Both experimental measurements and theoretical predictions pertaining to collision processes are frequently made in terms of cross sections.

The primary objective of this research has been the measurement of cross sections for the formation of fast, excited hydrogen atoms in the 3s, 3p, and 3d states by the impact of protons on gaseous targets. Impact energies ranged from 75 to 400 keV. The process of interest was the direct formation of these atoms by transfer of an electron from a target atom.

$$H^+ + X \rightarrow H^*(3s,\ 3p,\ \text{or}\ 3d) + X^+ \qquad (1)$$

Targets "X" of helium and of molecular nitrogen were used.

A process of secondary interest was the collisional destruction of excited atoms prior to their spontaneous radiative decay.

$$H^*(3s,\ 3p,\ \text{or}\ 3d) + X \rightarrow [H^+ + e] + [X] \qquad (2)$$

The brackets are used to indicate that the present experiments provided no information on the states of the post-collision products except for the fact that the H atom was no longer in the n=3 level. However, theoretical predictions[1] indicate that nearly all such collisions at the impact velocities of this experiment result in ionization of the hydrogen atom.

Various approximation methods have been developed to predict cross sections for the types of collisions described by equations (1) and (2). Born's approximation is expected to be of satisfactory accuracy provided that the impact velocities are sufficiently high. Calculations of this type have been made of the cross sections for capture of an electron from a helium atom by a fast proton.[2] The hydrogen atoms formed in these collisions may be in their ground state or in any excited state. Calculations and measurements have been made by a number of workers of cross sections for capture into the ground state and of the total cross sections for capture into any bound state,[3,4,5,6,7] for capture into the 2s and 2p excited states, and for a few other cases. A listing of measurements of excited state capture cross sections is provided in Chapter VI. Born approximation calculations have also been made of the cross section for formation of hydrogen atoms in the 3s, 3p, and 3d states by the impact of protons on helium.[2] These cross sections have been measured previously by other investigators[8,9,10,11] for a range of impact velocities which is, for the most part, below the range in which the Born approximation is valid. The impact velocities of the present experiment extend into a region where a more significant test of the theoretical predictions may be made.

It is argued that a detailed comparison of theory and experiment for the charge transfer formation of specific excited states may be carried out effectively for only the n=3 level. Measurements for states with $n \geq 6$, which have been made by field ionization techniques,[12,13,14,15] provide at best a sum of the cross sections for the different angular momentum states ℓ and often do not allow resolution of states with different principal quantum numbers n.[16,17] The features of the cross section for formation of a particular state $n\ell$ are frequently hidden in such a sum, and these experiments have therefore not provided very sensitive tests of theory. For states having $n \geq 4$, the stray fields commonly encountered in experimental systems are sufficient to cause Stark mixing of the sublevels, thereby destroying their separate identity. The formation of the n=2 level has been studied elsewhere (see Table 6), but the level, of course, includes only two values of ℓ. It is therefore concluded that the most significant, unambiguous test of theory must be carried out on the n=3 states.

It should be noted that a successful theoretical prediction requires both that the wave functions used should be accurate and that the approximations made in the calculation should be valid. The post-collision wave functions required in the calculation for electron capture on a helium target are all hydrogenic; there is no dispute as to the form of these functions. The prior-collision wave function is that of the two electron helium atom; the cross section predictions have been shown to be fairly independent of the form of this function.[18,19] It may be concluded that the comparison of experiment and theory for this case is a valid test of the theoretical approximation and is not

appreciably influenced by inadequacies of the wave function.

A knowledge of electron capture cross sections is important in a number of practical situations as, for example, in the design of a system for controlled fusion of hydrogen nuclei in which the plasma density is increased by injection of beams of highly excited hydrogen atoms into the containment device.[20,21] These cross sections are also relevant to the understanding of certain phenomena observed in natural auroras and in the complex situations which exist immediately after an atmospheric nuclear explosion. It was with these applications in mind that measurements were made with a target of molecular nitrogen in addition to those made with helium.

CHAPTER II

EXPERIMENTAL TECHNIQUE

The formation of excited H atoms in the 3s, 3p, and 3d states is detected by the quantitative measurement of the Balmer alpha photons emitted as the excited atoms decay to the n=2 level. The Balmer alpha (H_α) emission is in fact due to three transitions: 3s → 2p, 3p → 2s, and 3d → 2p. These all emit photons of essentially the same wavelength and are therefore detected simultaneously. Other means than spectroscopic separation must be employed if the three contributions to the H_α emission are to be separately identified.

At the high impact energies utilized in this experiment, the product of the projectile's velocity and the lifetime of the excited state is a length comparable with the dimensions of the apparatus. Therefore, in general, a projectile will move an appreciable distance from the point where it was excited before emitting a photon and decaying to a lower state. As a result, the intensity of emission from the projectiles is a function of the position along the flight path at which the observation is made and also of the lifetime of the emitting state. Measurement of the spatial variation of this emission intensity allows the contributions of the 3s, 3p, and 3d states to be separately identified and the populations of the three emitting states to be evaluated.

Two experimental arrangements are possible to handle this problem.

In the first, the photon emission from the H atoms is observed as the beam traverses the target gas. In the second, the beam traverses a gas cell of definite length where the electron capture occurs, and the emissions are observed from the H atoms after they emerge from the cell as they proceed through an evacuated flight tube.

For the present measurements it was decided to study the problem through the decay of excited projectiles as they traversed the target gas. This approach is discussed in the following section. The alternative method involving the observation of decay in an evacuated flight tube is discussed in the succeeding section in order that a comparison of the two methods may be made.

Observations in the Target Region

Consider first the experimental arrangement in which measurements are made of the intensity of photon emission from H atoms as they traverse the target region. Suppose that photons emitted in the decay of state j to a lower state k are detected. The state j has a lifetime τ_j, and the cross section for its formation by the mechanism of equation (1) is Q_j.

Initially the assumptions are made (1) that the population of state j by cascade from higher levels is sufficiently small that it may be neglected, and (2) that atoms are removed from state j only by the process of spontaneous emission. Then the relation between the population of the upper level j and the desired cross section Q_j may be developed in the following manner.

A current of F projectile ions per second is incident with a

velocity v (cm/sec) on a target which has a number density ρ (molecules/cc). Let x be distance measured along the beam axis from the point of entrance to the target region. Let n^*_j be the number of excited atoms in state j per unit length along the beam axis. During time interval dt, the incremental change in n^*_j from direct collisional formation and spontaneous radiative decay is given by

$$dn^*_j = F \rho Q_j \, dt - n^*_j \sum_{i<j} A_{j\to i} \, dt \tag{3}$$

Here $A_{j\to i}$ (sec^{-1}) is the transition probability for spontaneous decay of the state j to the state i. Since

$$\sum_{i<j} A_{j\to i} = \frac{1}{\tau_j} \, , \; x = vt, \text{ and } v = \frac{dx}{dt}$$

equation (3) may be rewritten as a function of x instead of time.

$$\frac{dn^*_j}{dx} = \frac{F \rho Q_j}{v} - \frac{n^*_j(x)}{v\tau_j} \tag{4}$$

If a further assumption is made that the proton beam current F is not significantly depleted in passing through the target region, the solution of equation (4) is given by

$$n^*_j(x) = F \rho Q_j \tau_j \left[1 - e^{-\frac{x}{v\tau_j}}\right] \tag{5}$$

All three of the assumptions made in arriving at this result will be subjected to further scrutiny (see Chapter III).

In general, the state j may decay by many paths to lower states i, only one of which ($j \rightarrow k$) is detected experimentally. Therefore, the number of photons detected corresponds to the fraction $\frac{A_{j\rightarrow k}}{\sum_{i<j} A_{j\rightarrow i}}$ and this fraction is known as the branching ratio.

Let J_{jk} be the number of photons emitted per second in the transition $j \rightarrow k$ from a segment of beam path whose center is at x and whose length is d. $J_{jk}(x)$ is then given by

$$J_{jk}(x) = A_{j\rightarrow k} \int_{x-\frac{d}{2}}^{x+\frac{d}{2}} n^*_j(x')\, dx' \qquad (6)$$

If d is much less than $v\tau_j$, the approximation may be used that

$$J_{jk}(x) = A_{j\rightarrow k}\, n^*_j(x)\, d \qquad (7)$$

The validity of this approximation for the present experiment is demonstrated in Chapter IV.

A detector which views the segment d of the beam path will produce a signal proportional to $J_{jk}(x)$. If the possibility of an anisotropic radiation pattern is, for the moment, ignored, the constant of proportionality will be the product of two factors: (1) the ratio of the solid angle ω subtended by the detector as seen from the point x to the total solid angle 4π, and (2) the absolute detection efficiency of the detector to photons incident upon it from transitions $j \rightarrow k$ occurring within d.

It is convenient to define a normalized emission function $G_{jk}(x)$ as the number of photons emitted per second in transition $j \rightarrow k$ at position x, per unit length of beam, per unit incident beam flux, per unit target density.

$$G_{jk}(x) \equiv \frac{J_{jk}(x)}{F\ \rho\ d} = Q_j \frac{A_{j\rightarrow k}}{\sum\limits_{i<j} A_{j\rightarrow i}} \left[1 - \exp\left(-\frac{x}{v\tau_j}\right)\right] \tag{8}$$

Since, in the present experiment, the Balmer alpha emission is due to three transitions, the observed emission function is a sum of three terms of the type given in equation (8).

$$G_{\alpha}(x) \equiv \frac{J_{\alpha}(x)}{F\ \rho\ d} = I_0 \left[1 - \exp\left(-\frac{x}{v\tau_0}\right)\right] + I_1 \left[1 - \exp\left(-\frac{x}{v\tau_1}\right)\right] \tag{9}$$

$$+ I_2 \left[1 - \exp\left(-\frac{x}{v\tau_2}\right)\right] + K$$

where

$$I_j = Q_j \frac{A_{j\rightarrow k}}{\sum\limits_{i<j} A_{j\rightarrow i}}$$

and a term K, independent of position, has been included to allow for contributions to the signal from collisionally induced target emission. The subscripts 0, 1, and 2 are used to indicate, respectively, the 3s, 3p, and 3d states. It happens that the 3s and 3d states can decay spontaneously only by the Balmer alpha transition and therefore the branching ratio $\frac{A_{j\rightarrow k}}{\sum\limits_{i<j} A_{j\rightarrow i}}$ for these states is unity. For the $3p \rightarrow 2s$ transition, this ratio is 0.118,[22] indicating that only 11.8 percent of the atoms in the 3p state decay by the emission of a Balmer alpha photon,

the rest by Lyman beta. Equation (9) represents a sum of three terms which increase exponentially with x toward an asymptote. Because the three lifetimes of the states are quite different, it is possible to compare the measured function $G_\alpha(x)$ with equation (9) and to evaluate the coefficients I_j. In this manner, the cross sections for the formation of the 3s, 3p, and 3d states may be measured using the different lifetimes to identify the three sublevels.

Observations in an Evacuated Flight Tube

A possible alternative would be to observe the decay of the population of excited states in the beam after emerging from a gas cell into an evacuated flight tube. In this case the intensity of emission from each state will simply decay exponentially with distance along the flight tube with a decay length characterized by the lifetime of the excited state. The population of the excited states in the emergent beam will be a function of the cell length L. The normalized emission function for the transition $j \rightarrow k$ expressed in terms of the distance x beyond the exit from the gas cell may be shown[8] to be given by the following equation.

$$G_{jk} = Q_j \frac{A_{jk}}{\sum_{i<j} A_{ji}} \left[1 - \exp\left(-\frac{L}{v\tau_j}\right)\right] \exp\left(-\frac{x}{v\tau_j}\right) \qquad (10)$$

Again the Balmer alpha line is in fact the sum of three contributions and its normalized emission function can be represented by the equation

$$G_\alpha(x) = I_o \left[1 - \exp\left(-\frac{L}{v\tau_o}\right)\right] \exp\left(-\frac{x}{v\tau_o}\right) \qquad (11)$$

$$+ I_1 \left[1 - \exp\left(-\frac{L}{v\tau_1}\right)\right] \exp\left(-\frac{x}{v\tau_1}\right)$$

$$+ I_2 \left[1 - \exp\left(-\frac{L}{v\tau_2}\right)\right] \exp\left(-\frac{x}{v\tau_2}\right)$$

where I_j has the same significance as before. This equation may be fitted to the observed emission function and the cross sections evaluated.

The two experimental configurations are complementary, each having different advantages and drawbacks. Observations made in the target region may be subject to interference from collisionally induced target gas emissions. These will be invariant with beam penetration through the gas and will require the inclusion of the constant term K in equation (9). Unless this constant is small in comparison with the other terms, it is impossible to evaluate the separate 3s, 3p, and 3d excitation cross sections with any accuracy. In particular, the interesting case of an H_2 target becomes quite impossible due to target emission. The approach of using a cell and an evacuated flight tube enhances the populations of the short-lived 3p and 3d states relative to the 3s population, which tends to dominate in the other configuration. This enhancement is possible because the 3p and 3d populations approach their equilibrium (maximum) values within a short distance (10 to 20 cm) of the entrance to the target region, whereas the population of long-lived 3s state reaches only 10 to 20 percent of its equi-

librium value in this distance. Cross sections for formation of these two short-lived states can therefore be more accurately measured. Within the target region of either experimental configuration, collisions of the type shown in equation (2) will affect the spatial dependence of the population of excited states. However, the use of an evacuated observation region eliminates the possibility, present with the first configuration, that collisions of this type can hinder the analytical separation of the observed Balmer alpha emission into its three separate contributions by altering the apparent lifetimes of the excited states. On the other hand, the gas cell approach requires care to ensure that the exit aperture from the cell does not intercept an appreciable fraction of the scattered projectiles. Furthermore, there is an uncertainty as to the "thickness" of a gas cell due to pressure gradients at the two apertures.

It was concluded that both techniques have their disadvantages, although these can be mitigated by proper tests. Agreement between data obtained by the two separate methods would give considerable confidence to the validity of experimental measurements. For the purposes of the present thesis, the method of observation of emission from the target region was adopted.

Apparatus

The source of incident protons for the present experiment was a one MeV Van de Graaff positive ion accelerator, which was equipped with a beam analyzing and stabilizing system. The incident proton energy was determined to within ± 2 keV by deflection through 90° in a regulated

magnetic field. Beam currents of 0.3 to 3.0 μA were typically employed.

The experimental apparatus is shown schematically in Figure 1 and photographically in Figure 2. The equipment required for the acquisition and recording of data is also indicated in the block diagram of Figure 3.

The incident proton beam was collimated to one-sixteenth inch diameter by two knife-edged orifices spaced six inches apart. A third orifice of larger diameter was suitably biased to collect secondary electrons. A fourth orifice in the form of a short (one-eighth inch) channel provided the limiting aperture between the collision chamber and the accelerator to inhibit the loss of target gas from the cell. This orifice had a diameter such that no particles which had traversed the first two apertures could be incident upon it, thereby reducing the possibility of secondary electrons and sputtered material entering the observation region.

The ion beam was monitored after traversing the collision and detection region on a deep parallel-plate Faraday cup assembly with an inclined end (Figure 4). Tests indicated that the application of suitable biases to parts of the beam collection system (C,D) resulted in complete suppression of secondary electrons and ions. Ion-beam currents were measured by an electronic microammeter, whose reading was transformed into a series of pulses with the aid of a voltage-to-frequency converter. The pulse frequency was proportional to the incicated current reading, and the pulses could be counted by a scaler for any desired length of time. This arrangement automatically integrated

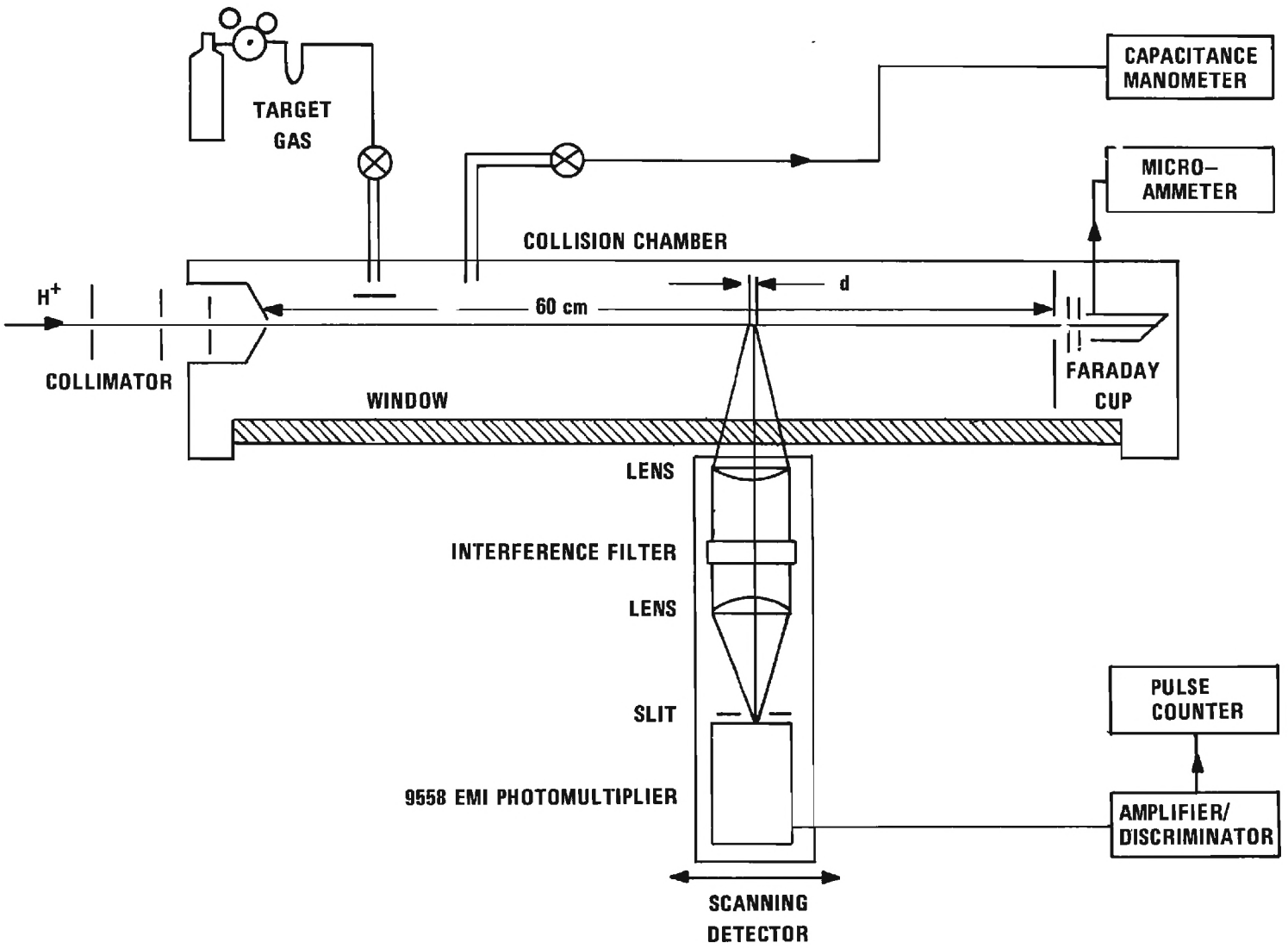

Figure 1. Schematic Diagram of the Apparatus for Measuring Emission in the Target Region.

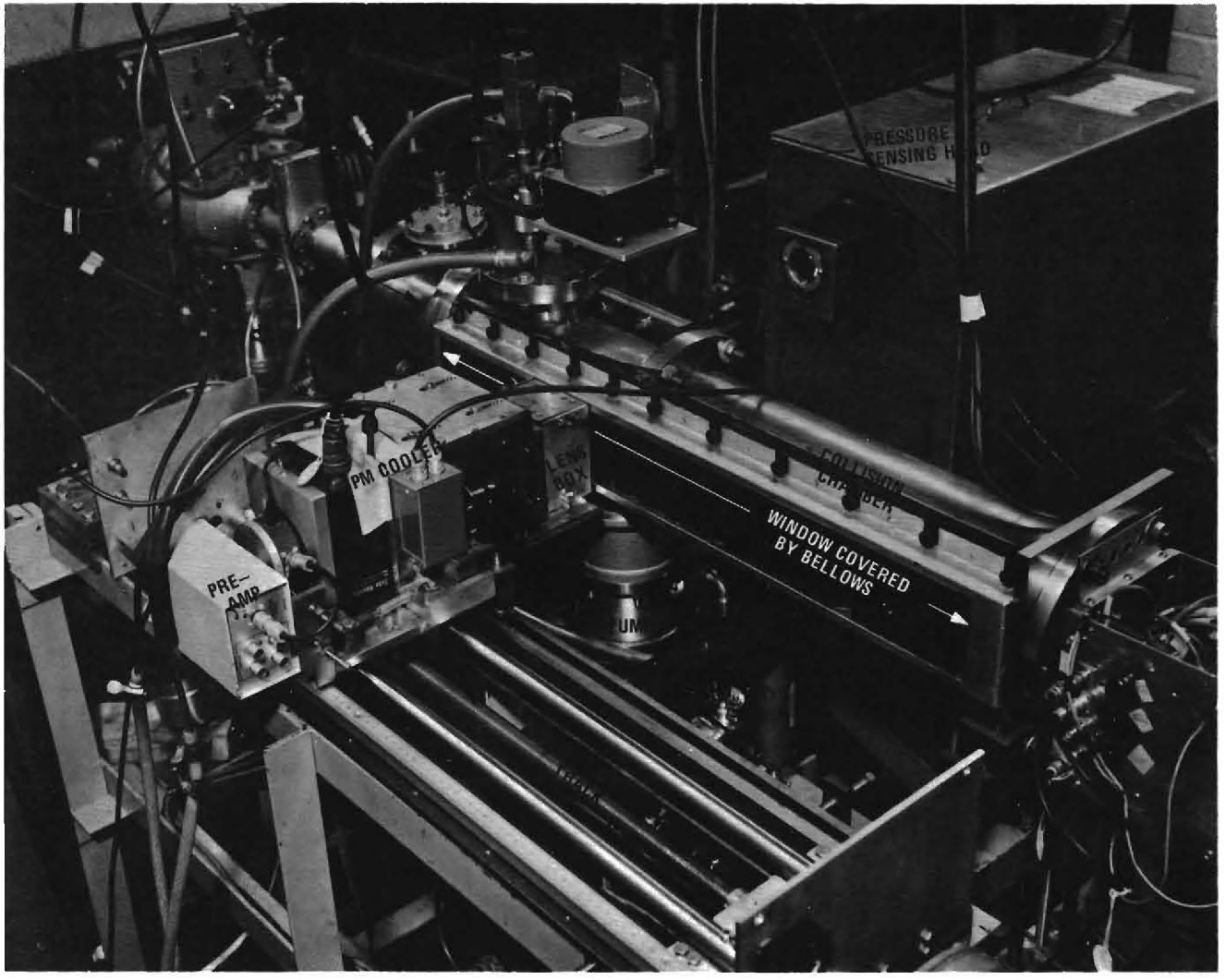

Figure 2. Photograph of Apparatus.

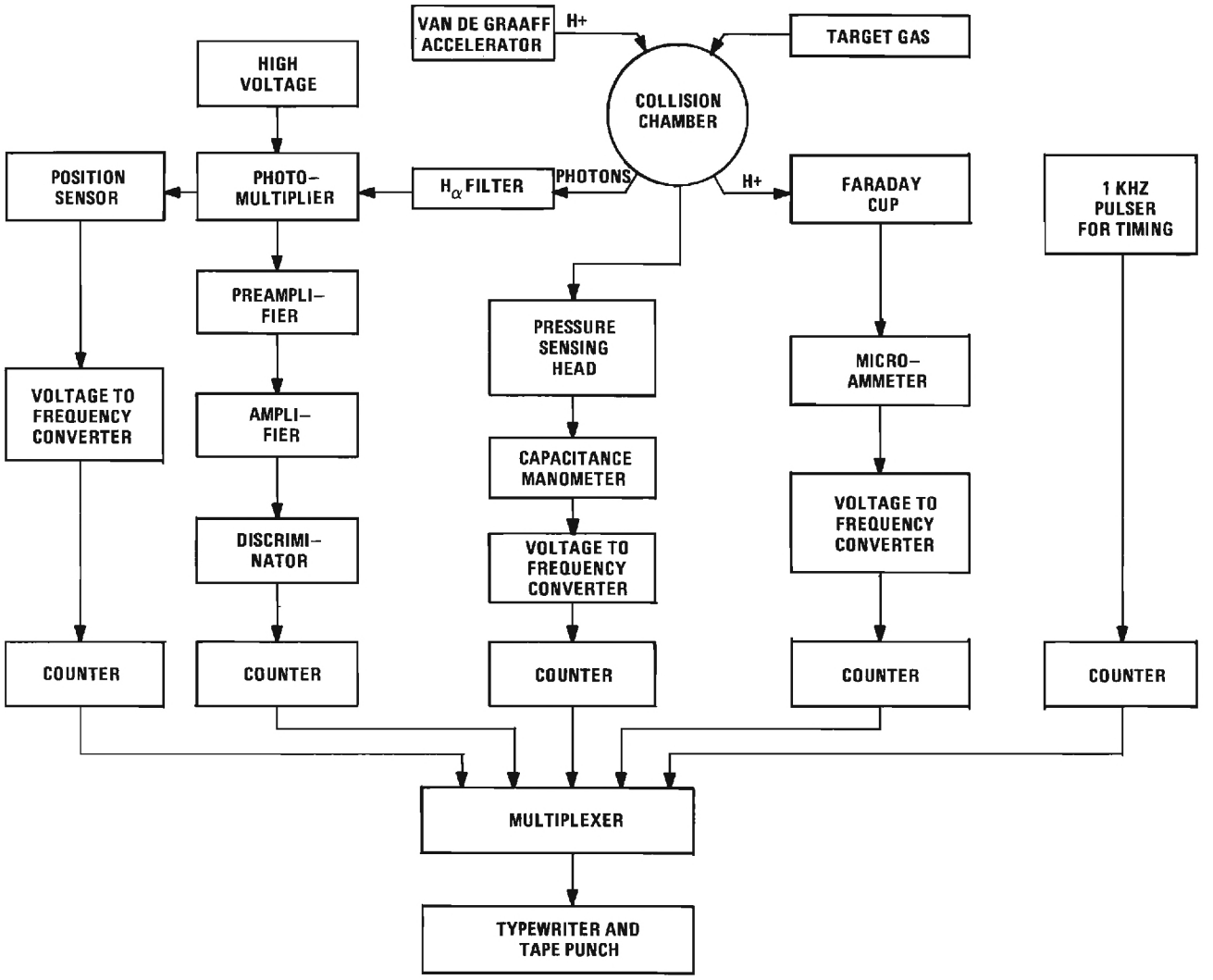

Figure 3. Block Diagram of Apparatus.

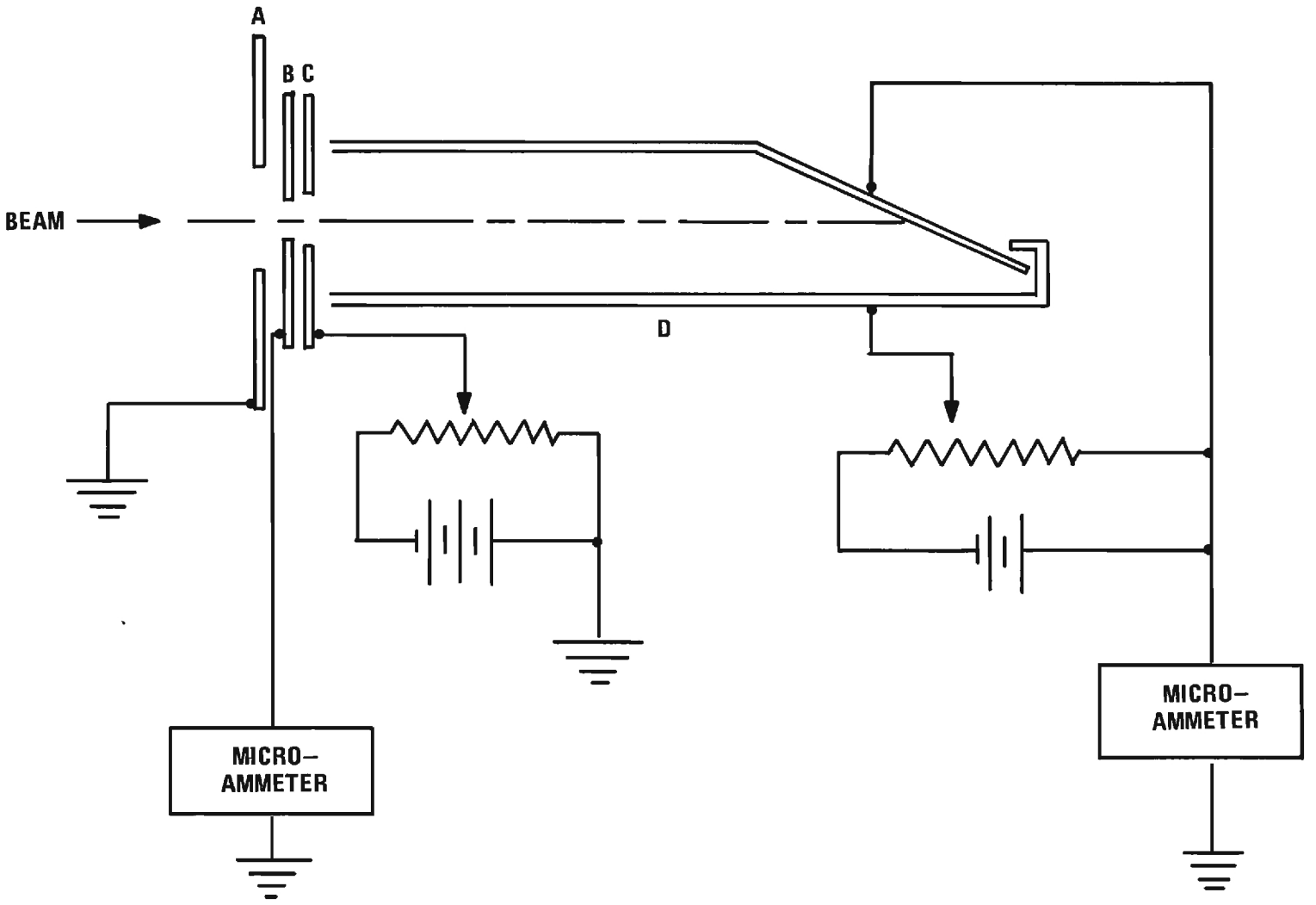

Figure 4. Schematic Diagram of Faraday Cup.

the ion current during the period the pulse counter was gated on.

It was possible for particles in the beam to be scattered in passing through the target by an angle sufficient to prevent their entrance into the Faraday cup. A simple device allowed this scattered portion of the beam to be monitored. A plate ("B", in Figure 4) was placed just in front of the entrance aperture (C) of the Faraday cup. The aperture in plate B was slightly the smaller of the two, so that all beam particles passing through it were certain to enter the Faraday cup. The current collected by plate B was monitored at all times and remained below one percent of the current collected by the Faraday cup. The emission of secondary electrons from B would cause indication of a current larger than the true scattered current. Therefore, it is certain that at least 99 percent of the beam was collected.

In addition, a grounded plate (A), having a large hole for the beam, was placed just in front of B to isolate the electrostatic fields of the Faraday cup and its associated electrodes from the collision region. Plate A thus prevented slow ions produced in the target from being attracted by the negative potentials and prevented these fields from having any effect on events occurring within the observation region.

The target gas was passed through a cold trap to remove any condensable materials and was leaked into the collision chamber. The purity of the helium used was stated by the manufacturer to be at least 99.999 percent and of the nitrogen 99.9 percent. The target gas pressure was monitored continuously by a capacitance manometer which

had been calibrated against a McLeod gauge (see Chapter IV). The pressure measurement of the manometer was converted into pulses in the same manner as the indication of beam current. Pressure measurements could then be recorded by a pulse counter for convenience in data handling.

A window of crown glass in one side of the collision chamber allowed a view of the entire beam path. The Balmer alpha detector could be moved along a machined track to measure emission intensity at any position along a 60 cm length of the flight path. Light emitted from a short segment of the beam was focussed at infinity by a lens, passed at normal incidence through an interference filter, and refocussed by a second lens to form an image of the beam segment on the face of an EMI 9558 photomultiplier tube. A slit placed just in front of the tube's face limited its view to a six mm segment of the beam. A survey was made of the point-to-point variations in sensitivity over the face of the tube, and its orientation was chosen such that the variation in sensitivity over the exposed portion was less than two percent. The photomultiplier was operated in the pulse mode, and its output was fed through a preamplifier, amplifier, and discriminator and counted by scaling equipment. Considerable care was taken to set the discriminator threshold at a level which gave the optimum signal-to-noise ratio. The photomultiplier was housed in a thermoelectric cooler in order to reduce its dark current. Typical dark currents amounted to five to 10 percent of the total pulse count. Tests showed that the dark current was invariant with small changes in the photomultiplier's operating temperature, which was typically -25°C. The dark current was measured frequently

and appropriate corrections were made in the data. A bellows covered the window in the collision chamber to prevent the entrance of stray light, but as an added precaution, the entire room was darkened during the collection of data. A backdrop covered with a homogeneous black coating of colloidal graphite was placed at the side of the beam opposite the Balmer alpha detector in order to eliminate the effect of internal reflections.

The absolute detection efficiency was determined by measurement of the intensity of emission of the Balmer alpha line from a target of molecular hydrogen under the impact of protons. The absolute cross section for this process was measured in an earlier experiment in this laboratory[23] with the aid of a tungsten filament standard lamp. Any unintentional loss or gain of light due to reflection, absorption, or inaccuracies in slit width would have equal effect on the measurement of fast particle emission and the target emission which was being used as the transfer standard. Such errors would therefore not affect the comparison. Errors arising from Doppler effects were considered, and appropriate corrections were made.

A simple arrangement was devised for electrical measurement of the position of the detector. This information was also recorded by a counter for convenience in data handling. A meter stick mounted beside the detector track provided a reference measurement of position. The detector was moved by an electric motor drive.

The collision chamber and the differential pumping chamber, which contained the collimating apertures, were constructed of type 304 stainless steel and assembled with Viton O-rings. The collimator,

Faraday cup, and backdrop assemblies were constructed of brass. The chambers were pumped separately by oil diffusion pumps equipped with liquid nitrogen traps. The oil used in these pumps was Dow-Corning number 705, which contains no hydrocarbons. The forelines were also equipped with cold traps to inhibit back-pumping of cracked hydrocarbons from the mechanical forepumps. Base pressures in the chambers were about 3×10^{-7} Torr. With target gas at operating pressure in the collision chamber, a pressure differential of about 100:1 was maintained across the entrance aperture of the collision chamber.

The operation of the entire experiment was, to a great extent, automated. The large quantity of raw data generated made this almost a necessity. In each set of data were 50-200 measurements of each of the following quantities: position of the detector, light intensity, target gas pressure, accumulated ion current, elapsed time. It was arranged that all of these quantities could be recorded digitally by pulse counters. A multiplexer read the counters serially at the end of each photon count, and the readings were recorded both by a teletypewriter and by a paper tape punch attached to it. Information on the punched tape was reproduced on computer cards by a tape-to-card converter in a form acceptable to Georgia Tech's Burroughs B-5500 computer. A program was written to calculate $G_\alpha(x)$ at each position x, to fit the appropriate equation to the reduced data, and to present the results both digitally and graphically. An example of the graphical presentation of one data set is shown in Figure 5. The best values of I_0, I_1, I_2, and K were determined in the fitting procedure according to the least squares criterion, and the three electron capture cross sections were calculated from these coefficients.

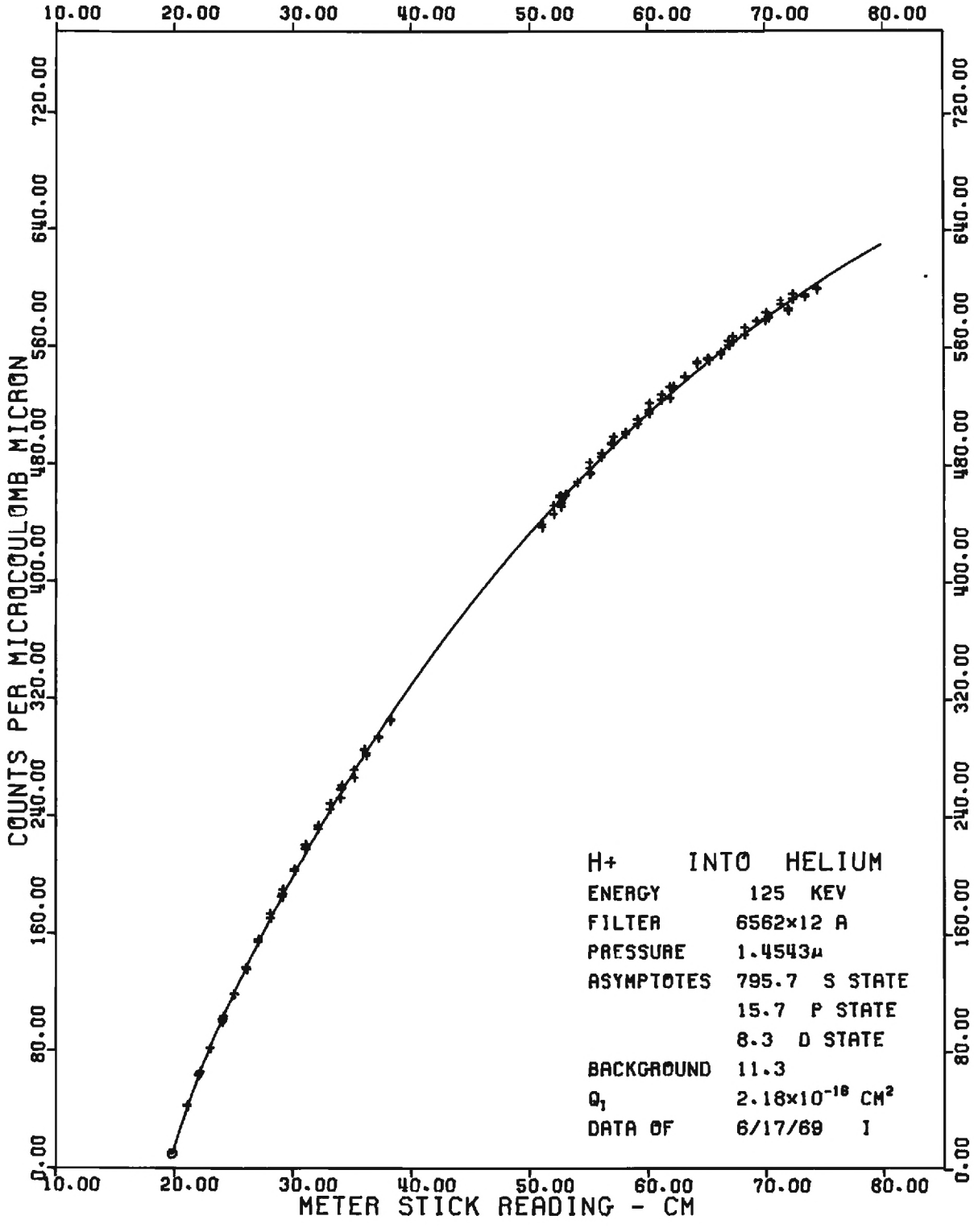

Figure 5. Typical Set of Data.

CHAPTER III

DETERMINATION OF THE CROSS SECTIONS

The primary objective of the experiment is the measurement of the cross sections for the formation of the 3s, 3p, and 3d excited states of H by electron capture. The experimental method involves first the separation of the Balmer alpha emission by the time-of-flight technique discussed in Chapter II; second, the measurement of the relative variation of each component as a function of energy; and third, the normalization of the data set to a standard of emission in order to provide absolute cross sections.

Although the techniques to accomplish this, outlined in Chapter II, are apparently quite simple, there are many second order processes which tend to distort the measurement. There are additional processes which populate and depopulate the excited states; these include cascade, collisional destruction, and multiple collisions of projectiles. There is a possibility that the emission is anisotropic. Doppler shift of the emission from the projectile results in the effective sensitivity of the optical system exhibiting a dependence on projectile velocity. The influence of all these processes must be assessed in order to arrive at the final cross section results.

Measurement and Analysis of the Normalized Emission Function

In order to determine the three charge exchange cross sections Q_{3s}, Q_{3p}, and Q_{3d}, for a given target and energy, the normalized emission

function for the Balmer alpha line was measured at many positions x along the chamber. Initially, attempts were made to analyze the data according to equation (9). It became immediately clear for targets of both helium and nitrogen that the cross section for charge exchange into the 3s state was at least an order of magnitude larger than the 3p and 3d cross sections throughout the range of impact energies utilized, 75 to 400 keV. However, the values of the cross sections obtained by fitting equation (9) to the data suffered a systematic variation with the density of the target gas, and it appeared that this occurred as a result of multiple collisions of particles in the beam.

The Influence of Multiple Collisions

In the derivation of equation (9) were several simplifying assumptions whose validity is subject to question. It was assumed

(1) that atoms were removed from the n=3 states only by the process of spontaneous radiative emission;

(2) that the proton beam current was not significantly depleted in passing through the target region;

(3) that contributions to the population of n=3 states by cascade from higher levels were negligible (this assumption does not involve multiple collisions and will be discussed separately (see page 36)).

Collisional Destruction of Excited Atoms. The failure of the first assumption was apparent from the following observation. At values of x much larger than both $v\tau_{3p}$ and $v\tau_{3d}$ the contributions to the H_α emission from the short-lived 3p and 3d states had essentially reached their equilibrium values. Any variation in photon emission

$G_\alpha(x)$ with x in this region must have been due to variation of only the 3s contribution, and equation (9) reduced to

$$G_\alpha(x) = I_0 \left[1 - e^{-\frac{x}{v\tau_{3s}}}\right] + I_1 + I_2 + K \qquad (12)$$

The data consistently showed that as x increased, the 3s contribution approached its equilibrium value more rapidly than equation (12) predicted and that the rate of approach increased with target gas density. This behavior was evidently due to collisional destruction of 3s state atoms before they decayed by spontaneous emission of a photon.

The collisional destruction of excited atoms (equation (2)) has the effect of reducing the effective lifetime of the excited state by the factor $(1 + v\tau\rho Q_i)^{-1}$. Again ρ is the density of the target gas whereas Q_i is the cross section for the destruction process. As a result it is necessary to alter equation (12) by adding the term ρQ_i to the exponent. (The same term must be added to each of the exponents of equation (9). In addition, there are some corresponding changes to the factors I_0, I_1, and I_2 of equations (9) and (12).) If ρQ_i is much smaller than $1/v\tau$, it may be neglected and the analysis of the experiment is as previously described (equation (9)). In principle, this can be achieved by making the target density ρ sufficiently small. In practice the cross section Q_i is very large and it is not possible to reduce the target density sufficiently to remove the influence of the destruction process without causing unacceptable reductions in signal intensity. High statistical accuracy is a necessary requirement for

the deconvolution of the emission variation into three parts using the characteristic lifetimes of the three relevant excited states. This accuracy cannot be achieved with low signal levels.

The process of collisional destruction is a mechanism of some considerable intrinsic interest. It was decided that the best method of handling its influence on the present experiments was to measure it directly.

The collisional destruction cross section Q_i may be obtained for the 3s state by analysis of data for which x is sufficiently large that 3p and 3d contributions to the emission have essentially reached their equilibrium values. Practically speaking, this means x must be at least 12 to 25 cm. Neglecting cascade and beam neutralization, the data should fit an equation of the form

$$G_\alpha(x) = I_o \left\{1 - \exp\left[-\left(\frac{1}{v\tau_{3s}} + \rho Q_i\right) x\right]\right\} + I_1 + I_2 + K \qquad (13)$$

that is, an exponential rise plus terms invariant with x. Q_i may be determined by adjusting its value to obtain the best possible fit of equation (13) to the data according to the least squares criterion.

It is interesting to note that, in determining Q_i, no calibration of a detector is required. It is necessary to know only v, τ_{3s},[‡] and ρ and to obtain the apparent decay length $\left[\frac{1}{v\tau_{3s}} + \rho Q_i\right]^{-1}$ from the data.

[‡] τ_{3s}, the lifetime of the 3s state of H, is well known from the theory of the H atom,[24] and the value has been confirmed experimentally.[25,26,27] The value used in the present work was obtained from reference 22.

Collisional destruction of atoms in the 3p and 3d states also tends to accelerate the approach to equilibrium of their populations, but because these states have much shorter lifetimes, the effect is much less pronounced.

Beam Neutralization. The failure of assumption (2) concerning the variation of the proton flux with x was evident from the reduction in proton flux collected by the Faraday cup when a target gas is introduced into the evacuated collision chamber. Its failure was also apparent from a consideration of the loss and production of protons in the beam at any point x along the beam axis, where x is the distance from the entrance aperture of the collision cell. Since the beam flux is affected principally by two processes, charge transfer and collisional ionization, the change of proton flux in distance dx at x is given by

$$\frac{dn_+(x)}{dx} = - n_+(x)\ \sigma_c \rho + n_o(x)\ \sigma_s \rho \qquad (14)$$

where

$n_+(x)$ is the number of protons at x per unit length of beam,

$n_o(x)$ is the number of neutral atoms at x per unit length of beam, $n_+(0) - n_+(x)$,

σ_s is the total stripping cross section for neutral atoms,

σ_c is the total electron capture cross section for protons,

ρ is the target gas density.

The solution of equation (14) is then given by

$$n_+(x) = \frac{n_+(0)}{\sigma_s+\sigma_c} \left\{\sigma_s + \sigma_c \exp\left[-\rho(\sigma_s+\sigma_c)\, x\right]\right\} \qquad (15)$$

where $n_+(0) = \frac{F}{v}$ is the linear density of the incident proton beam. Calculations based on equation (15) utilizing values of σ_s and σ_c measured by Barnett, et al.[6,7] indicate that in the present experiment the proton flux may be reduced in the worst cases by as much as 18 percent in passing through a helium target (1.5×10^{-3} Torr at 75 keV impact energy) or as much as 20 percent in a nitrogen target (0.6×10^{-3} Torr at 75 keV).

Excitation of Neutrals. Still another process resulting from beam neutralization can have a significant effect on the measurements: collisional excitation of ground state neutrals formed in the beam. It is difficult to assess the importance of this process because neither theoretical predictions nor experimental measurements of the pertinent cross sections have been found in the literature for the present collision targets, helium and nitrogen. If calculations by Bates and Griffing[28] for H(1s) on H(1s) can be taken as any indication of the magnitudes to be expected, the process may have only a small effect on the measured emission intensities, but some verification is necessary.

Analysis Employed

A model for the experiment must then account for the following processes:

(1) charge transfer into the three excited states of interest

$H^+ + X \rightarrow H^*(3s, 3p, \text{or } 3d) + X^+$ cross sections Q_{3s}, Q_{3p}, Q_{3d} (collectively referred to as $Q_{3\ell}$);

(2) spontaneous decay of the excited atoms

$H^*(3s, 3p, \text{or } 3d) \rightarrow H(1s, 2s, \text{or } 2p) + h\nu$ lifetimes τ_{3s}, τ_{3p}, τ_{3d} (collectively $\tau_{3\ell}$);

(3) collisional destruction of the excited atoms

$H^*(3s, 3p, \text{or } 3d) + X \rightarrow H(n \neq 3) + X$ cross sections $Q_{i,3s}$, $Q_{i,3p}$, $Q_{i,3d}$ (collectively $Q_{i,3\ell}$);

(4) attenuation of the proton beam

$H^+ + X \rightarrow H^o + X^+$ cross section σ_c

$H^o + X \rightarrow H^+ + e + X$ cross section σ_s

resulting in a proton density given by equation (15) and a neutral atom density given by

$$n_o(x) = \frac{n_+(0)}{\sigma_s+\sigma_c} \sigma_c \left\{1 - \exp\left[-\rho(\sigma_s + \sigma_c)\, x\right]\right\} \qquad (16)$$

(5) excitation of the neutral component of the beam to the excited states of interest

$H^o + X \rightarrow H^*(3s, 3p, \text{or } 3d) + X$ cross sections $Q_{x,3s}$, $Q_{x,3p}$, $Q_{x,3d}$ (collectively $Q_{x,3\ell}$).

The differential equation governing the linear density of excited atoms in the 3s state, n^*_{3s}, is given by

$$\frac{dn^*_{3s}(x)}{dx} = - n^*_{3s}(x) \left(\frac{1}{v\tau_{3s}} + \rho Q_{i,3s}\right) + n_+(x)\, \rho Q_{3s} + n_o(x)\, \rho Q_{x,3s} \qquad (17)$$

Similar equations can be written for the 3p and 3d populations. Using equations (15) and (16) for $n_+(x)$ and $n_o(x)$, the solution of (17) is

$$n^*_{3s}(x) = \frac{n_+(0)\ \rho}{\sigma_s+\sigma_c} \left\{ \left[\frac{\sigma_s Q_{3s} + \sigma_c Q_{x,3s}}{\frac{1}{v\tau_{3s}} + \rho Q_{i,3s}} + \frac{\sigma_c\ (Q_{3s} - Q_{x,3s})}{\frac{1}{v\tau_{3s}} + \rho Q_{i,3s} - \rho(\sigma_s+\sigma_c)} \right] \right. \tag{18}$$

$$\times \left[1 - e^{-\left(\frac{1}{v\tau_{3s}} + \rho Q_{i,3s}\right)x} \right] - \frac{\sigma_c\ (Q_{3s} - Q_{x,3s})}{\frac{1}{v\tau_{3s}} + \rho Q_{i,3s} - \rho(\sigma_s+\sigma_c)}$$

$$\left. \times \left[1 - e^{-\rho(\sigma_s+\sigma_c)x} \right] \right\}$$

Populations of the 3p and 3d states are given by similar equations with "3s" replaced by "3p" and "3d". The equation for total photon emission including a position-independent contribution from the target or background gas is

$$J_\alpha(x) = \{A_{3s\to 2p}\ n^*_{3s}(x) + A_{3p\to 2s}\ n^*_{3p}(x) \tag{19}$$

$$+ A_{3d\to 2p}\ n^*_{3d}(x)\}\ d + KF\ \rho d$$

and

$$G_\alpha(x) = \left\{ \frac{1}{v} \frac{1}{(\sigma_s+\sigma_c)} \right\} \left\{ \sum_{\ell=0}^{2} A_{3\ell\to 2\ell'} \left(Q_{3\ell} \left[\frac{\sigma_s}{\frac{1}{v\tau_{3\ell}} + \rho Q_{i,3\ell}} \right. \right. \right. \tag{20}$$

$$\left. \left. \left. + \frac{\sigma_c}{\frac{1}{v\tau_{3\ell}} + \rho Q_{i,3\ell} - \rho(\sigma_s+\sigma_c)} \right] + Q_{x,3\ell}\ \sigma_c \right.$$

(continued)

$$\times \left[\frac{1}{\frac{1}{v\tau_{3\ell}} + \rho Q_{i,3\ell}} - \frac{1}{\frac{1}{v\tau_{3\ell}} + \rho Q_{i,3\ell} - \rho(\sigma_s+\sigma_c)} \right] \Bigg)$$

$$\times \left[1 - e^{-\left(\frac{1}{v\tau_{3\ell}} + \rho Q_{i,3\ell}\right)x} \right] - \sigma_c \left[\sum_{\ell=0}^{2} A_{3\ell \to 2\ell'} \left(\frac{Q_{3\ell} - Q_{x,3\ell}}{\frac{1}{v\tau_{3\ell}} + \rho Q_{i,3\ell} - \rho(\sigma_s+\sigma_c)} \right) \right]$$

$$\times \left[1 - e^{-\rho(\sigma_s+\sigma_c)x} \right] \Bigg\} + K$$

Equation (20) replaces equation (9) as a description of the experiment. Note that the three exponential terms of equation (9) have remained except that each decay length $v\tau$ has been replaced by $(\frac{1}{v\tau} + \rho Q_i)^{-1}$ and the expressions corresponding to I_0, I_1, and I_2 have become more complicated. Also a fourth exponential term has appeared. Equation (9) expresses the limiting value of $G_\alpha(x)$ as ρ the target gas density approaches zero.

The unknown quantities in equation (20) are:

(a) the cross sections for charge exchange into n=3 states Q_{3s}, Q_{3p}, and Q_{3d};

(b) the cross sections for collisional destruction of n=3 state atoms $Q_{i,3s}$, $Q_{i,3p}$, and $Q_{i,3d}$;

(c) the cross sections for excitation of ground state neutrals into n=3 states $Q_{x,3s}$, $Q_{x,3p}$, and $Q_{x,3d}$;

(d) a term to allow for collisionally induced target emission, K.

In principle, it is possible to analyze data of $G_\alpha(x)$ versus x according

to an equation of the form of equation (20) to obtain coefficients of the four exponentials, the constant K, and, by treating the lifetimes of the exponentials as unknowns, the three cross sections $Q_{i,3\ell}$. Variations with ρ in the values of the coefficients could be used to determine the $Q_{3\ell}$ and $Q_{X,3\ell}$. However, the accuracy and reproducibility of the data are not nearly sufficient to obtain a reliable fit with such a large number of parameters. The statistical uncertainties obtainable in practical counting times render such a complex analysis hopeless.

In order to obtain useful information from the experiment, a substantial reduction must be made in the number of unknowns to be determined by analysis of the data. This may be done either by the elimination of parameters from the analysis through the use of relationships among them, or by altering the experimental conditions (e.g., reducing the target gas density) so that a simpler model describes adequately the operation of the experiment.

The cross sections Q_{3s}, Q_{3p}, and Q_{3d} clearly cannot be eliminated from equation (20) since their determination is the primary purpose of the experiment.

K can, in principle, be measured separately by allowing the detector to view the emission at such an angle to the beam that emissions from the fast atoms are Doppler shifted out of the band of wavelengths detected. Instrumental difficulties have rendered this approach impractical. However, in this experiment K is quite small and its presence is not a serious handicap to the analysis. It has been retained in the equation and is determined by analysis of the data.

Bates and Walker[1] predict that the cross sections $Q_{i,3s}$, $Q_{i,3p}$, and $Q_{i,3d}$ are approximately equal. Collisional destruction has a substantial effect on the apparent decay length of the 3s state, and it is possible to measure $Q_{i,3s}$. Note, however, that the destruction cross sections appear in equation (20) only in the sums $\frac{1}{v\tau_{3\ell}} + \rho Q_{i,3\ell}$. Although the data indicate that $\rho Q_{i,3s}$ is comparable in magnitude to $\frac{1}{v\tau_{3s}}$, the term appears to be much smaller than $\frac{1}{v\tau_{3p}}$ and $\frac{1}{v\tau_{3d}}$. Moderate errors in $Q_{i,3p}$ and $Q_{i,3d}$ therefore have little effect on the analysis of data for other unknowns. This is a further justification for replacing $Q_{i,3p}$ and $Q_{i,3d}$ by $Q_{i,3s}$ as Bates and Walker suggest. These three cross sections will henceforth be denoted simply as Q_i.

The determination of the cross sections $Q_{x,3\ell}$ presents a difficult problem. In principle, the coefficients of the first three exponentials in equation (20) could be found for two values of ρ, and two simultaneous equations could be solved for each pair of cross sections $Q_{3\ell}$ and $Q_{x,3\ell}$. The accuracy of the data is not sufficient to allow this.

The literature apparently does not contain measurements or predictions of $Q_{x,3s}$ for targets of helium or nitrogen in the energy range of the present experiment. It is possible, however, to assess by an auxiliary experiment described in the following section the effect of neglecting both the last term of equation (20), and the terms containing $Q_{x,3\ell}$ in the coefficients of the first three exponentials. The auxiliary experiment showed that these terms are not significant to the mathematical description of the principal experiment. The data were therefore analyzed according to equation (21) which omits these terms,

$$G_\alpha(x) = \left\{ I_o \left[1 - e^{-\left(\frac{1}{v\tau_{3s}} + \rho Q_i\right)x} \right] + I_1 \left[1 - e^{-\left(\frac{1}{v\tau_{3p}} + \rho Q_i\right)x} \right] \right. \qquad (21)$$

$$\left. + I_2 \left[1 - e^{-\left(\frac{1}{v\tau_{3d}} + \rho Q_i\right)x} \right] + K \right.$$

where

$$I_\ell = \frac{A_{3\ell \to 2\ell'} Q_{3\ell}}{v(\sigma_s+\sigma_c)} \left[\frac{\sigma_s}{\frac{1}{v\tau_{3\ell}} + \rho Q_i} + \frac{\sigma_c}{\frac{1}{v\tau_{3\ell}} + \rho Q_i - \rho(\sigma_s+\sigma_c)} \right]$$

(ℓ=0 for 3s state, ℓ=1 for 3p state, and ℓ=2 for 3d state)

to determine values of Q_{3s}, Q_{3p}, Q_{3d}, K, and Q_i.

An additional argument is presented in Appendix II which makes plausible on other grounds the negligibility of these terms containing $Q_{x,3\ell}$.

Checks on the Adequacy of the Analysis

A calculation based on equation (20), utilizing estimated values of the unmeasured cross sections, has shown that the normalized Balmer alpha emission function, $G_\alpha(x)$, varies almost linearly with target density at any given position x, for target pressures of a few microns or less. Therefore, measurements of $G_\alpha(x)$ can be made at several values of ρ and at two values of x chosen to be sufficiently large that contributions to the H_α emission intensity from p and d states have essentially reached their asymptotic values, and the value of

$$\lim_{\rho \to o} G_\alpha(x) = \frac{1}{Fd} \lim_{\rho \to o} \left(\frac{J_\alpha(x)}{\rho} \right)$$

can then be obtained by extrapolating linearly to zero pressure at each position, x. Taking the limit as $\rho \to o$ of equation (20) for x in the

range described above yields

$$\lim_{\rho \to 0} G_{\alpha}(x) = Q_{3s} \left[1 - e^{-\frac{x}{v\tau_{3s}}}\right] + K' \qquad (22)$$

where

$$K' = A_{3p \to 2s}\, \tau_{3p} Q_{3p} + Q_{3d} + K \qquad (23)$$

Values of Q_{3s} and K' can be obtained from two equations at the two different values of x. Measurements of Q_{3s} and K' made in this way by extrapolation to zero target density agree well with the values obtained from data at finite pressures and analyzed according to equation (21). This agreement demonstrates that the approximations required to obtain equation (21) are justified.

Assessment of Cascade

In addition to direct collisional excitation, the 3s, 3p, and 3d states may also be populated by cascade from higher levels. This fact has two important consequences. First, the measured cross section will then not represent only the formation of the state by collision but will include a component due to cascade. Secondly, and perhaps more important, the dependence of emission intensity on distance will be different for atoms formed in n=3 states through cascade than for atoms formed directly. The cascade population will be dependent on both the lifetime of the parent level of the cascade transition and also the lifetime of the n=3 state that is populated. This second problem might invalidate the analysis of the separate cross sections which uses a deconvolution technique based on the assumed values of 3s, 3p, and 3d state lifetimes.

The population of higher n states may be estimated by taking the present measurements of the 3s, 3p, and 3d state cross sections and scaling them to higher n states assuming that cross sections for a given angular momentum substate decrease as n^{-3}. This general rule is well established[29,30] by theory and serves well for an approximate assessment of the problem. Because of the branching ratios for decay of higher states, the population of the n=3 level by cascade from higher np and nd states is very small and will influence the data by an amount that is smaller than the statistical reproducibility of the measurements. There is no method by which one can reasonably estimate the population of higher nf states. However, all theoretical predictions suggest that it is far less than for the corresponding nd state. Therefore, it too will be neglected. The only cascade contribution of any significance is from the ns states into the 3p level.

The 4s state is the largest cascade contributor to the Balmer alpha emission both because the cross section for its formation is larger than for any other cascade contributor and because the fraction of the 4s population decaying into the 3p (42 percent)[22] is larger than for any other contributor. The linear density $n^*_{4s\rightarrow 3p}(x)$ of the 3p state due to cascade from the 4s state is given by

$$n^*_{4s\rightarrow 3p}(x) = \left(\tfrac{3}{4}\right)^3 Q_{3s}\, A_{4s\rightarrow 3p}\, \tau_{4s}\, \rho F\, \tau_{3p} \qquad (24)$$

$$\times \left[\left(\frac{1}{\frac{\tau_{4s}}{\tau_{3p}} - 1}\right) e^{-\frac{x}{v\tau_{3p}}} + \left(\frac{1}{\frac{\tau_{3p}}{\tau_{4s}} - 1}\right) e^{-\frac{x}{v\tau_{4s}}} + 1\right]$$

where $(\frac{3}{4})^3 Q_{3s}$ is the estimated cross section for formation of atoms in the 4s state.

Except at small x where the population vanishes asymptotically, $n^*_{4s\rightarrow 3p}(x)$ varies approximately as $1 - \exp(-\frac{x}{v\tau_{4s}})$, the manner characteristic of the long-lived 4s state population. (τ_{4s} = 226.6 nsec, τ_{3p} = 5.273 nsec.)[22] An estimate of the intensity of Balmer alpha emission due to 4s→3p cascade may be made with the help of equation (24). Expressed as a percentage of the emission from atoms formed by capture directly into the 3s state, this intensity varies from zero at small x to 1.6 percent at the largest x observable in the present apparatus (at 75 keV, where this problem is at its worst), and, in principle, to 2.1 percent at x sufficiently large for the populations to reach equilibrium values. Balmer alpha emission due to cascade from the 5s state, expressed in the same way varies from zero at small x to 0.5 percent at the largest x observable in this apparatus, asymptotically to 0.8 percent as $x\rightarrow\infty$. From 6s, the figures are zero, 0.2 percent, to 0.4 percent. Summing the contributions for all n at the largest observable x gives a total estimated contribution only about 2.5 percent as large as the emission from the 3s state.

When a term allowing for the estimated 4s cascade contribution to the 3p population is added to equation (21), the value of Q_{3s} obtained from analysis of data is reduced by about 1.5 percent. The other cross sections (including Q_i) are not affected. Since at the energies of this experiment the n^{-3} rule is only an estimate (although measurements by Hughes, et al.[31] of Q_{3s} and Q_{4s} near 100 keV tend to confirm

it), no cascade correction is applied to the data. However, the rule does allow an estimate to be made of the uncertainty in the cross section measurements due to this source. This error is evaluated in Chapter IV and proves to be rather small in comparison with other known errors.

Effects of Polarization

Emission from the 3p and 3d states may exhibit polarization. The polarization fraction is related to the population of the different magnetic quantum number sub-levels, and is zero if these levels are all equally populated. It may be shown that the collisionally induced emission will be anisotropic if polarization is present. A measurement of emission at one angle does not allow the determination of a cross section unless correction is made for this anisotropy.

Much of the research discussed in this report has been directed at the $3s \rightarrow 2p$ emission which is unpolarized and therefore emitted isotropically. No attempt has been made to measure polarization for the $3p \rightarrow 2s$ and $3d \rightarrow 2p$ emissions. Because of the small signal intensity from these states the statistical accuracy would be so poor as to render the measurement meaningless. Consequently, it is not known whether the emissions are isotropic. However, upper and lower bounds can be placed on the degree of polarization possible in these emissions, and a full discussion of the resulting uncertainties in the 3p and 3d capture cross sections is presented in Chapter IV.

It should be noted that any polarization which may exist in the p and d state radiations can have no effect on the separation of the contributions of the three parent states to the detected radiation.

The neglect of an anisotropic radiation pattern will, however, cause error in the values of the 3p and 3d capture cross sections interpreted from these contributions. If the polarization of these emissions varies with energy, its neglect will result in error in the energy dependence of the p and d cross sections. This error is evaluated in Chapter IV and its largest possible value is shown to be small compared with other uncertainties.

Stark Effect Mixing

The experiment is designed to determine cross sections for the formation of the 3s, 3p, and 3d states using the lifetimes of these states for identification. However, if an electric field is applied to the excited atoms, the energy levels will be perturbed by the Stark effect, and "mixing" of certain states will cause changes in the effective lifetimes of the excited states.[24] There is a danger that stray fields in the apparatus may cause this effect.

The states which are most vulnerable to mixing are those having the same value of the total angular momentum quantum number, j. For the n=3 level, the critical fields, i.e., the minimum fields which will cause full mixing, are 58 volts/cm for the $3s_{\frac{1}{2}}$ and $3p_{\frac{1}{2}}$ states and 1.9 volts/cm for the $3p_{\frac{3}{2}}$ and $3d_{\frac{3}{2}}$ states.[24]

Clearly, the weak field Stark effect may distort the operation of the experiment. It would be impossible to correct the data for the effects of substantial stray fields since they would probably vary in space and time. In principle, it would be possible to design a field-free experiment, but this would entail a considerable increase in com-

plexity. Instead, some simple precautions were taken to reduce the possibility of Stark mixing, and a test was made to determine whether mixing was affecting the experiment.

The collimation system was designed so that the beam could not strike any part of the gas cell aperture as it entered the target region. (Hughes, et al. reported inconsistencies in their early results[8,9] because of the lack of such a precaution.) The only surfaces exposed to the beam were clean, conducting surfaces, so that accumulation of a static charge was unlikely. The window through which the H_α radiation was observed was an exception to this statement, but it was located at the largest practicable distance from the beam.

Finally, Stark plates were installed in the observation region so that electric fields could be intentionally applied to the beam. The application of these fields showed that the 3s state was not affected by any fields which might conceivably exist in the apparatus. It was not possible to prove conclusively that the 3p and 3d states, which made only small contributions to the total H_α emission, were completely free from mixing because the data were subject to random fluctuations from other sources. However, there was no detectable evidence that these states were mixed by fields which existed in the apparatus, and it will be assumed in the presentation of data that there was no mixing.

Assessment of the Effect of Doppler Shift on the Sensitivity of the Optical System

The arrangement of the detector of Balmer alpha (H_α) photons is indicated in Figure 1. Light emitted within a 12° cone centered at 90°

to the beam axis is focused at infinity by a lens, filtered by an H_α interference filter having either a 12 Å or a 30 Å full width at half maximum, focused by a second lens to form an image of the beam on the cathode of an EMI 9558 photomultiplier tube. A mask restricts the photomultiplier's view to a six mm length of beam. This length is sufficiently short to insure that no significant error is introduced by assuming that the emission intensity per unit length of beam at the point of intersection of the beam axis and the optical axis of the detector assembly is the observed intensity divided by the length of beam within view.

The high velocity of the radiating hydrogen atoms (0.012 c to 0.03 c for 75 to 400 keV energies where c is the velocity of light) causes significant Doppler shifts in the wavelength of the observed radiation. Although the optical axis of the detector is at 90° to the beam axis, the finite aperture of the optical system admits radiation emitted at angles from 78° to 102° to the beam axis. The increase in wavelength of H_α radiation observed at exactly 90° to the beam axis due to relativistic time dilation varies from 0.5 Å at 75 keV to 2.1 Å at 400 keV, and the Doppler spread of emissions accepted by the finite aperture ranges from 34 Å at 75 keV to 80 Å at 400 keV.

Because the Doppler shifts vary with the velocity of the emitting particle, the effective sensitivity of the detector varies with the impact energy of the incident protons. It should be emphasized that this dependence has no effect on measurements of the relative magnitudes of Q_{3s}, Q_{3p}, and Q_{3d} at a given energy, but it will affect the apparent dependence on energy of these cross sections. The following technique

has been developed to correct for this variation in sensitivity.

Consider H_α radiation emitted at an angle θ to the beam by a hydrogen atom at point P (Figure 6).

Let $E(v,\theta)$ be the H_α emission per unit solid angle at θ, per unit length of beam for incident particles having velocity v.

$E(v,\theta)d\omega$ is then the emission into solid angle $d\omega$ per unit length of the beam.

$\int_\omega E(v,\theta)d\omega$ is the total emission per unit length of beam path.

Neglecting polarization, $E(v,\theta)$ is independent of θ and may be written as $E(v)$, but the observed wavelength λ varies with θ as

$$\lambda = \lambda_o \frac{1 + \frac{v}{c}\cos\theta}{\left(1 - \frac{v^2}{c^2}\right)^{\frac{1}{2}}} \tag{25}$$

where $\lambda_o = 6562.8$ Å, the H_α wavelength.

Let $T(\theta)$ be the transmittance per unit solid angle of the lens system (excluding the filter) to light of the H_α wavelength emitted at an angle θ to the beam. For the small range of wavelengths passed by the filter, $T(\theta)$ can be assumed independent of wavelength.

Let $t(\lambda)$ be the transmittance of the filter to normally incident light of wavelength λ.

Let $D(\lambda)$ be the detection efficiency of the photomultiplier to light of wavelength λ.

The signal (photomultiplier output) per unit length of beam due to photons passing through solid angle $d\omega$ located at angle θ is then

$$dS = E(v)\ T(\theta)\ t(\lambda)\ D(\lambda)\ d\omega \tag{26}$$

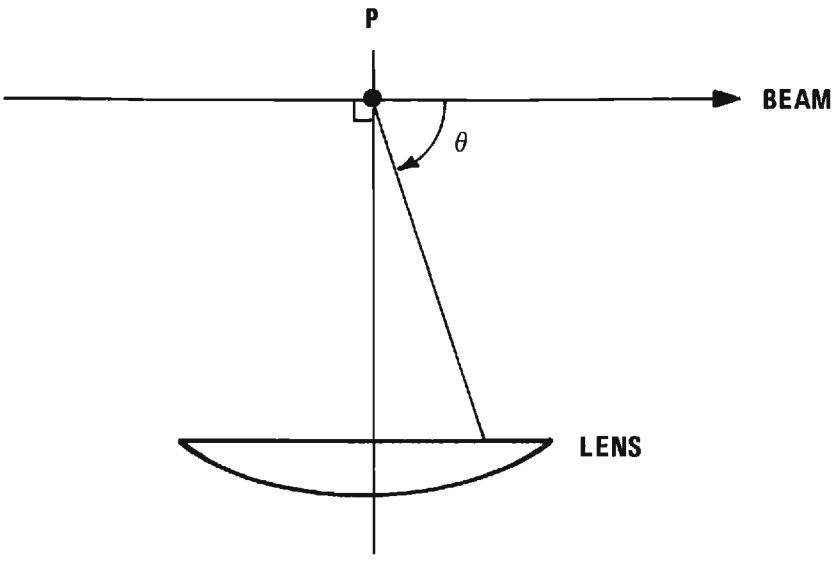

Figure 6. Geometry of the Optical Aperture.

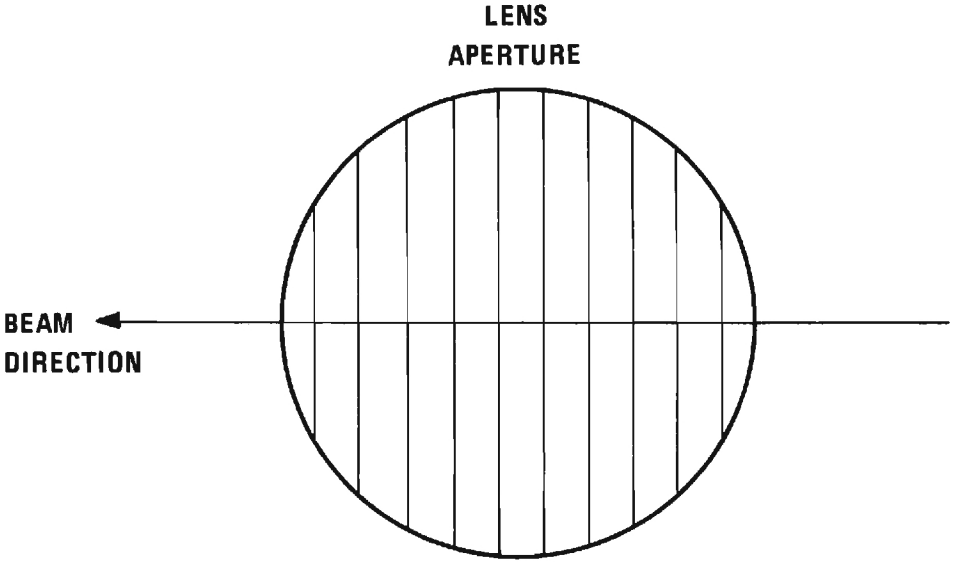

Figure 7. Division of the Optical Aperture into Segments for Measurement of T(θ). (See text.)

Integrating over the entire optical aperture

$$S(v) = \int E(v)\ T(\theta)\ t[\lambda(v,\theta)]\ D[\lambda(v,\theta)]\ d\omega \qquad (27)$$

where, in accordance with equation (25), $\lambda = \lambda(v,\theta)$.
Filter transmittance $t(\lambda)$ has been measured with the aid of broad band light source and a Jarrell-Ash 0.5 meter Ebert-Fastie spectrometer. Wavelength calibration of the spectrometer was accomplished with the aid of a hydrogen arc lamp, which emits a strong Balmer alpha line.

The variation in $D(\lambda)$ from its value at the H_α wavelength is only about $\pm$ 4 percent over the wavelength range of interest and is approximately linear, according to the manufacturer. For the present purposes, D(6562.8 Å) may be arbitrarily set equal to unity, and the manufacturer's data used to estimate its dependence on λ. Small errors in estimating this dependence will not have a significant effect on the results.

$T(\theta)$ at the H_α wavelength has been measured in the following way. The circular aperture of the optical system has been divided into eleven parts by ten equally spaced imaginary chords perpendicular to the ion beam direction (Figure 7). A diaphragm having a long rectangular aperture was placed between the lenses to stop all light except that passing between adjacent chords. In this way, only the light emitted within a small range of angles θ was admitted to the detector. $\int T(\theta)d\omega$ has been measured for each of the eleven parts, using as an emission source the H_α radiation from a molecular hydrogen target under the impact of 150 keV protons. The reaction making the principal contribution to the H_α radiation was the dissociative excitation of the target:

$$H^+ + H_2 \rightarrow H^+ + H^*(n=3) + H \tag{28}$$

Since the emitting particles were formed from the target molecules, they had low velocities and the wavelength of radiation was independent of θ. Emission from fast H atoms formed by electron capture into the n=3 states was of negligible intensity compared to the target emission. Eleven values of $W_k \equiv \int_k T(\theta)d\omega$ were thereby measured for the eleven parts of the aperture. If W_k is normalized so that $\sum_{k=1}^{11} W_k = 1$, then W_k becomes, in effect, the fraction of the optical aperture represented by part k.

θ is not exactly constant along each chord since the locus of points forming the intersection of a cone of constant θ with the plane of the aperture is actually a hyperbola, but within the area defined by the circular aperture, the error (less than 0.2° in θ) in approximating the hyperbolae by the chords causes negligible error in the results.

The signal ΔS_k due to photons passing through the k^{th} part of the aperture is, then

$$\Delta S_k = E(v)\ W_k\ t(\lambda_k)\ D(\lambda_k) \tag{29}$$

where $\lambda_k = \lambda(v,\theta_k)$, (30)

θ_k representing the mean value of θ in segment k.

Let $$t(\lambda) = t(\lambda_o)\ \alpha(\lambda) = t_o\alpha(\lambda) \tag{31}$$

and $$D(\lambda) = D(\lambda_o)\ \beta(\lambda) = D_o\beta(\lambda) \tag{32}$$

where α and β now represent only the variations in t and D from their values t_o and D_o for $\lambda = \lambda_o$.

Then $$\Delta S_k = E(v)\ W_k\ t_oD_o\ \alpha(\lambda_k)\ \beta(\lambda_k) \tag{33}$$

The total signal is $S(v) = \sum_{k=1}^{11} \Delta S_k$. (34)

The efficiency η of the detector may be defined as

$$\eta(v) \equiv \frac{S(v)}{E(v)} = t_o D_o \sum_k T(\theta_k)\ \alpha(\lambda_k)\ \beta(\lambda_k) \tag{35}$$

Two H_α filters have been used in the measurements and their transmission characteristics are shown in Figure 8. $\eta(v)$ has been arbitrarily normalized to a value of unity for the narrower filter for v=0, and the function is given for each of the filters in Figure 9.

In order to test the validity of the foregoing procedures, direct measurements of the eleven values of ΔS_k were made. H_α emission was produced through electron capture by 150 keV protons incident on a target of helium. The signal from this source was measured for each of the eleven segments of the optical aperture. Satisfactory agreement was obtained with the calculations of equation (29).

Calibration

Absolute calibration of the measured cross sections has been accomplished by comparison of H_α emission intensities obtained from the charge exchange process with those obtained from the dissociative excitation of molecular hydrogen:

$$H^+ + H_2 \rightarrow H^+ + H^*(n=3) + H \tag{36}$$

The absolute cross section for emission of the H_α line in this reaction was measured previously[23] in this laboratory and has been used as a transfer standard. The emitting atoms in this process have low velocities,

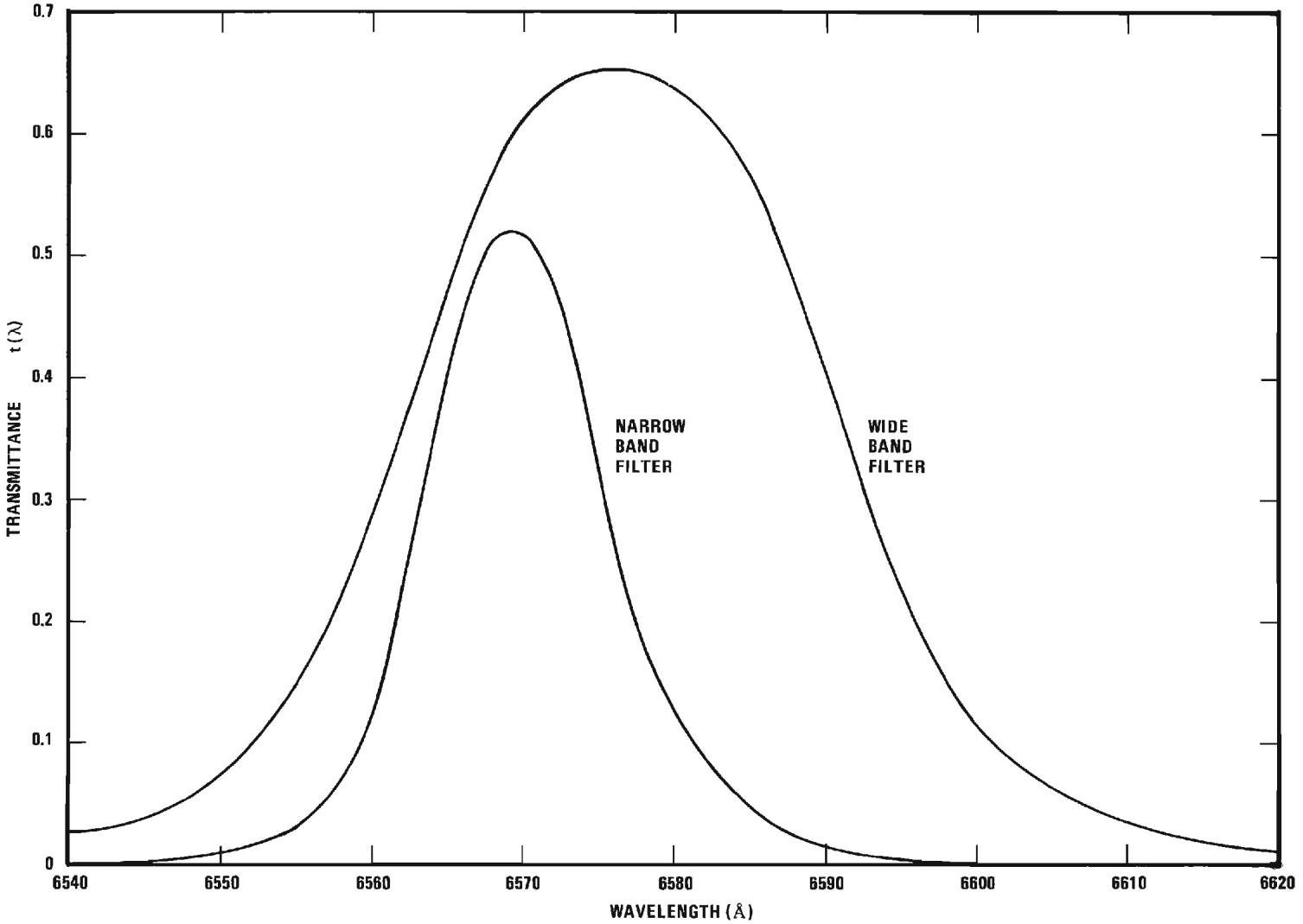

Figure 8. Pass Band Characteristics of the Interference Filters.

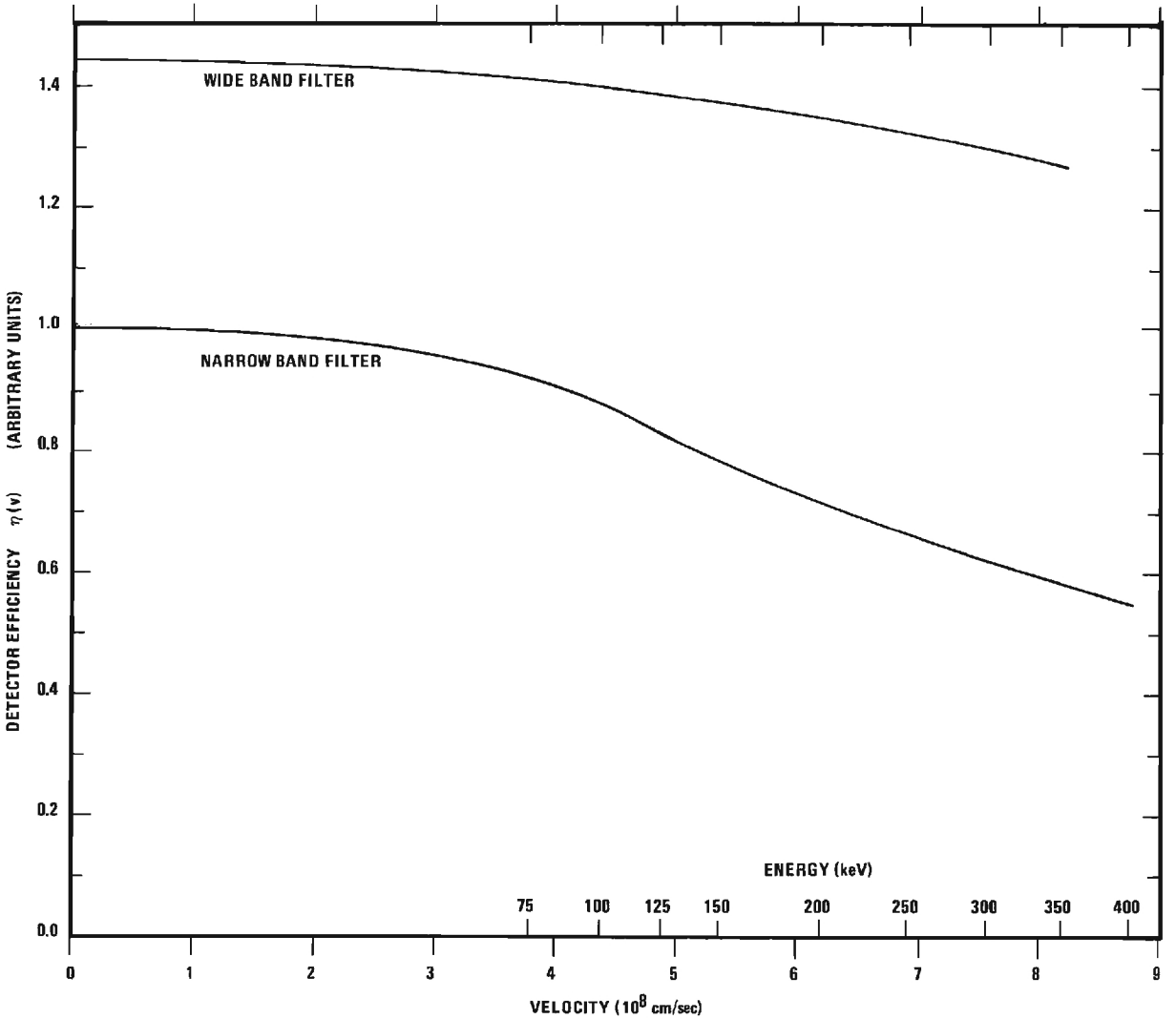

Figure 9. Relative Detection Efficiency of the Balmer Alpha Detector as a Function of the Velocity of the Emitting Atom.

and since Doppler effects in this case are negligible, the expression for the efficiency of the detector reduces to

$$\eta(0) = t_o D_o \sum_k T(\theta_k) \tag{37}$$

In determining absolute charge exchange cross sections for particles traveling with velocity v, only these ratios of detector efficiency are required:

$$\frac{\eta(v)}{\eta(0)} = \frac{\sum_k T(\theta_k)\ \alpha(\lambda_k)\ \beta(\lambda_k)}{\sum_k T(\theta_k)} \tag{38}$$

t_o and D_o drop out of the ratio, and only the variations of t and D with wavelength enter into the calculation.

CHAPTER IV

EXPERIMENTAL UNCERTAINTY

Three distinct types of possible error produce uncertainty in the present measurements. Uncertainties of a statistical nature are inherent in microscopic physical processes, and such errors scatter the measured values randomly about the true values. Other random variations in the apparatus produce a similar scatter of the measured values of cross sections, but those of a systematic nature may cause errors in one direction only.

Statistical Fluctuations and Other Random Variations

The rates at which events occur on an atomic scale fluctuate in a manner beyond the control of any experiment. As the number of events in an observation increases, the relative size of these fluctuations, from one observation to another, decreases and the observed rate approaches a long-term average. The effect of these statistical fluctuations on a given observation could, in principle, be reduced to insignificance by making observations over a sufficiently long period of time. However, practical limitations are imposed by the long-term stability of measuring instruments, particularly those in which continuous variables are processed electronically.

Several microscopic processes occurred in the present experiment and were responsible for random variations in the measurement of each cross section. Such processes were the initial formation of excited H

atoms, the subsequent spontaneous decay or collisional destruction of the excited atoms, the detection of emitted photons by the photomultiplier tube with the generation of detectable output pulses, and the spontaneous generation of spurious "dark current" pulses within the photomultiplier itself.

In addition to the fluctuations in rates of these microscopic processes, the data were affected by fluctuations in the measuring devices: drifts of the zero point and sensitivity of the pressure sensor, the beam current sensor and the detector's position sensor, and short-term variations in the sensitivity of the photon detector. These errors were treated as random rather than systematic because the directions of the drifts (which were small and were corrected frequently during the collection of each set of data) appeared to be random in direction and therefore had a random effect in scattering the individual data points. A practical way of relating the combined effect of these random variations and statistical fluctuations to variations in the resulting cross sections is to note the degree of reproducibility of the cross section measurements from one set of data to another.

Random Uncertainty in the Collisional Destruction Cross Sections

Measurements of Q_i were made by fitting an equation of the form

$$G_\alpha(x) = I_o \left[1 - e^{-\left(\frac{1}{v\tau_{3s}} + \rho Q_i\right)x}\right] + K' \qquad (39)$$

to a set of measured values of $G_\alpha(x)$, adjusting the values of I_o, Q_i, and K' to obtain the best fit according to the least squares criterion. K' corresponds to $I_1 + I_2 + K$ of equation (13)(see page 27).

Data were restricted to that region of x where contributions to the Balmer alpha emission from the short-lived 3p and 3d states had essentially reached their asymptotic values. Any change in emission intensity with position was then due to a change in the intensity of only the 3s state emission, and the fitting procedure determined the effective decay length for this state $(1/v\tau_{3s} + \rho Q_i)^{-1}$. An uncertainty in a measurement of this length resulted in an uncertainty in Q_i magnified by the ratio of $1/v\tau_{3s} + \rho Q_i$ to ρQ_i. The larger ρQ_i could be made in comparison to $1/v\tau_{3s}$, the more accurate was the measurement of Q_i. For this reason, greater reliance has been placed on the measurements of Q_i made at the higher target densities.

If the assumption is made, following Bates and Walker's suggestion,[1] that Q_i is essentially independent of the angular momentum quantum number, ℓ, then Q_i may be determined by an alternative analysis of the data. Data for $G_\alpha(x)$ may be fitted to an equation of the form

$$G_\alpha(x) = I_0\left[1 - e^{-(\frac{1}{v\tau_{3s}} + \rho Q_i)x}\right] + I_1\left[1 - e^{-(\frac{1}{v\tau_{3p}} + \rho Q_i)x}\right] \qquad (40)$$

$$+ I_2\left[1 - e^{-(\frac{1}{v\tau_{3d}} + \rho Q_i)x}\right] + K$$

where I_0, I_1, I_2, K, and Q_i are treated as unknowns. No restrictions need be placed on the range of x for which data are taken. Satisfactory agreement was obtained between values of Q_i determined in this way and those determined by the previous method, except at energies above 200 keV for a target of helium; under these conditions, Q_i is comparatively small, and the statistical scatter in the data caused a large

scatter in the determinations of Q_i.

Greater reliance has been placed on the determinations of Q_i made using equation (39) because the untested assumption concerning the dependence of Q_i on ℓ is not required.

The values of Q_i indicated in Figures 16 and 17 (see Chapter V) were determined by passing a smooth curve through weighted averages of the determinations made using equation (39). The set of error limits shown in Table 1 include all but one of those determinations and are indicated on the figures by error bars.

Table 1. Random Uncertainty in Q_i

Impact Energy	for a Helium Target	for a Nitrogen Target
75 - 125 keV	± 40%	± 40%
150 - 168 keV	± 65%	± 40%
200 - 400 keV	± 70%	+150% - 60%

Random Uncertainty in the Electron Capture Cross Sections

Measurements of Q_{3s} in helium made at two or three different pressures (within the range of 1 to 3 x 10^{-3} Torr) remained within four percent of the mean in all cases but one. For nitrogen, the extreme values of Q_{3s} (made within the pressure range of 2 to 6 x 10^{-4} Torr) were no more than 12 percent from the mean at all energies except the two highest, for which weak signals produced an unusually large scatter in the raw data.

In some of the results there appeared the suggestion of a weak dependence on ρ of the measured values of Q_{3s}. If the trend is real, it could result from the neglect of the excitation of ground state neutral atoms formed in the beam. Since the variations which suggested this dependence were no larger than the random fluctuations in the data, it is impossible to attach any significance to this observation. It did, however, serve to suggest the need for a test of the adequacy of the equation used to analyze the data.

To perform this test, several measurements of Q_{3s} were made by determining experimentally $\lim_{\rho \to o} G_{\alpha}(x)$ in the manner described on page 35. Values of Q_{3s} obtained from these extrapolations were free of any effects of the excitation of neutrals in the beam and free as well of the effects of collisional destruction of excited atoms. These determinations of Q_{3s} agreed well with the mean values obtained from the scans made at finite pressures. This fact confirms that the measurements of Q_{3s} obtained from scans at finite pressures were not affected significantly by the neglect of neutral excitation or by errors in Q_i.

An uncertainty in Q_i, or, more precisely, an uncertainty in the effective decay length $(1/v\tau + \rho Q_i)^{-1}$, does, of course, cause an associated uncertainty in the corresponding value of the capture cross section. However, the same random variations which produce uncertainties in the effective decay lengths produce the random variations in the measurements of the capture cross sections. Therefore, this source of uncertainty in decay length should not be considered an independent cause of uncertainty in Q_{3s}, Q_{3p}, and Q_{3d}.

Systematic Errors

Systematic Error in Target Gas Density

The density of the target gas was determined by measuring its pressure with a capacitance manometer. The temperature of the gas was assumed to be that of the collision chamber. Thermal equilibrium was assured because the construction of the tube through which the target gas passed upon entering the collision chamber required that each molecule make several collisions with its walls after expansion through the inlet valve.

The capacitance manometer was calibrated against a trapped McLeod gauge. Since the response of the capacitance manometer is independent of the nature of the gas whose pressure is being measured, the calibration was done with hydrogen in order that the error in the McLeod readings due to the Ishii effect[32,33] be at a minimum. The McLeod gauge was operated first at room temperature and then at about -10°C to reduce the streaming of mercury into the trap. A correction was made in the latter case for thermal transpiration[34] resulting from the difference in temperature between the pressure vessel and the refrigerated McLeod gauge. The sensing head of the capacitance manometer was usually operated at an elevated temperature, and the thermal transpiration resulting from this temperature gradient was also taken into account.

It is estimated that the uncertainty in target density during the experiment was no more than ± 6 percent for pressures exceeding 4×10^{-4} Torr and no more than ± 8 percent for pressures below 4×10^{-4} Torr.

Systematic Error in Impact Velocity

The uncertainty in v, the projectile velocity, resulting from an estimated ± 2 keV uncertainty in the energy of the projectiles entering the collision chamber is no more than ± 1.3 percent at 75 keV, decreasing to ± 0.5 percent for energies above 200 keV.

Systematic Error in Beam Current

Error in the measurement of the proton beam current which enters the collision chamber can be classified as follows:

(1) error originating in the collection of the beam,

(2) error in the current measuring device,

(3) inaccurate assessment of the effects of beam neutralization.

The ion beam was collected by a Faraday cup, which has been described in Chapter II. Tests indicated that the biases applied to the beam-collection system resulted in complete suppression of secondary electrons and ions. Less than one percent of the beam was scattered in passing through the collision chamber by such an angle that it did not enter the Faraday cup. This fact was demonstrated by the device already described for monitoring the scattered beam. It is therefore certain that at least 99 percent of the ion beam was collected (see page 19).

The collected current was monitored by a Keithley micro-microammeter, which was calibrated against an accurate current source. Error in the ammeter was estimated to be no more than ± 2 percent.

The analysis of data required a knowledge of the beam current entering the collision chamber. Because a portion of the beam was neutralized in passing through the target, a correction was necessary in order to obtain this initial current from the collected current. The

relevant total cross sections for charge transfer (σ_c) and stripping (σ_s) have been measured by Barnett, et al.[6,7] with uncertainties of ± 15 percent and ± 10 percent, respectively. The uncertainty in the beam current correction resulting from these uncertainties and the uncertainty in the target density was ± 3 percent for helium, ± 4 percent for nitrogen in the worst cases (75 keV, highest ρ), and dropped rapidly with increasing energy to less than ± 1 percent for energies of 150 keV or more.

The total uncertainties in the capture cross sections due to possible errors in beam measurement are given in Table 2.

Table 2. Uncertainty in the Capture Cross Sections Due to Uncertainty in the Beam Current

Impact Energy	for a Helium Target	for a Nitrogen Target
75 - 125 keV	+ 5% - 6%	+ 6% - 7%
150 - 400 keV	+ 3% - 4%	+ 3% - 4%

The effects of errors in σ_s and σ_c are not confined to the correction in beam current since these cross sections appear elsewhere in equation (21) used for analyzing data. However, these terms appear in both the numerator and the denominator, and errors in their values tend to cancel. The resulting uncertainties in capture cross sections are only about ± 1 percent at low energies and are negligible for energies of 150 keV or more.

Systematic Error from Doppler Effects

Because of Doppler effects, the apparent sensitivity of the Balmer alpha photon detector was a function of the velocity of the emitting particles, and the variation of sensitivity was determined in the manner described on page 41. The uncertainty in signal strength, and therefore in the capture cross section values, due to possible error in the correction for this effect is estimated in the following table.

Table 3. Uncertainty in the Capture Cross Sections Due to Uncertainty in the Correction for Doppler Effects

Impact Energy	Helium	Nitrogen
75 - 150 keV	± 1.3%	± 1.3%
168 - 400 keV	± 1.3%	± 3.3%

Systematic Error Due to the Finite Observation Length, d

Although the view of the photomultiplier tube included a six mm length of beam, it was assumed in analyzing the data that the observed signal strength was that appropriate to the center point of the portion of the beam within view. The error due to this assumption was always less than 0.2 percent--almost always much less--and is therefore considered negligible. Any inaccuracy which may have existed in measurement of the slit width did not produce error in measurements of the cross sections, since the detector was calibrated by a comparison method (see page 21).

Systematic Error Due to Variations in Sensitivity Over the Photomultiplier Face

Because of the slight divergence of the beam as it penetrated the target and because of the possibility of a slight misalignment between the beam and the track along which the photomultiplier traveled, it was necessary to insure that the sensitivity of the photomultiplier tube was constant over the exposed portion of its face. Tests revealed that, if the tube was suitably masked and properly oriented, the variations in sensitivity of its exposed face were no more than two percent from one extreme to the other. Appropriate precautions were taken, and tests in situ indicated that the error in the cross section measurements from this source was probably less than ± 2 percent.

Systematic Error in the Boundary of the Target Region

Because of the continuous effusion of gas out of the beam inlet hole, the target region cannot be said to have a sharp boundary. However, the escaping gas was pumped away rapidly (the pressure dropped by a factor of about 100 within a few millimeters), and an effective boundary plane could be established. Its position was determined in two ways: from a calculated density profile of the gas in the boundary region and by an experimental method. The density profile was determined theoretically for the geometry of this experiment on the assumption of molecular flow conditions, and the location of an effective boundary was calculated on the basis of this profile. The effective boundary was located experimentally by extrapolating a graph of H_α emission intensity versus target penetration to zero intensity. When an H_2^+ beam was substituted for the proton beam, it was observed that, at small x, the intensity of H_α

emission increased much more rapidly with target penetration, apparently because a larger proportion of atoms was formed in the 3p and 3d excited states. Because of the steeper slope, the extrapolation could be made with less uncertainty in x than was possible with the use of a proton beam. Measurements made under different conditions varied no more than 0.8 mm from the mean or from the position calculated from the gas density profile. It is therefore estimated that the error in position of this effective boundary is less than ± one mm, and the resulting uncertainty in the cross sections is as shown in Table 4.

Table 4. Uncertainty in the Capture Cross Sections Due to Uncertainty in the Boundary of the Target Region

Impact Energy	Q_{3s}	Q_{3p}	Q_{3d}
75 - 168 keV	± 0.2%	± 5%	± 2%
200 - 400 keV	± 0.1%	± 3%	± 1%

Systematic Error Due to Polarization

If the radiation emitted from a source is polarized, the radiation is not emitted isotropically. Since no meaningful polarization measurements could be made in the present experiment, it is not possible to correct for any anisotropy in the radiation pattern. However, an assessment of the maximum possible error resulting from the assumption of an isotropic pattern can be made.

Polarization is defined as

$$P = \frac{I_{\parallel} - I_{\perp}}{I_{\parallel} + I_{\perp}} \tag{41}$$

where $I_{\parallel}$ and $I_{\perp}$ are the intensities of the radiations having their electric vectors respectively parallel to and perpendicular to the beam direction, provided that the direction of observation is perpendicular to the beam. For an observation made in this direction the true cross section Q_T is related to the apparent cross section Q_A by the equation

$$Q_T = \frac{3 - P}{3} Q_A \tag{42}$$

Radiation from H atoms in an s state is unpolarized and is therefore emitted isotropically. No error results in Q_{3s} from this source. However, radiation from atoms in p and d states will, in general, be polarized.

The polarization of radiation from H atoms has been treated extensively by Percival and Seaton.[35] Their expression for the polarization of 2p→1s radiation (which holds approximately for 3p→2s radiation[36]) is

$$P = \frac{Q_0 - Q_1}{2.375\ Q_0 + 3.749\ Q_1} \tag{43}$$

where Q_0 and Q_1 are, respectively, the cross sections for populating the $m_\ell = 0$ and $|m_\ell| = 1$ states. Without a knowledge of the ratio Q_0/Q_1, only the extremes of P can be calculated. These will result if either Q_0 or Q_1 is zero, and therefore

$$-.267 \leq P \leq .421 \tag{44}$$

The resulting uncertainty in Q_{3p} is + 9 percent, - 14 percent.

Hughes, et al.[9] have derived the expression analogous to equation (43) for the polarization of radiation in the 3d→2p transition:

$$P = \frac{57(Q_0 + Q_1 - 2Q_2)}{119\ Q_0 + 219\ Q_1 + 162\ Q_2} \tag{45}$$

where Q_0, Q_1, and Q_2 are, respectively, the cross sections for formation of the $m_\ell = 0$, $|m_\ell| = 1$, and $|m_\ell| = 2$ states. Again only the extremes of P can be found without a knowledge of the ratios $Q_0:Q_1:Q_2$. The extremes of P occur when the linear momentum transfer is along the axis of quantization, in which case $Q_1 = Q_2 = 0$, or when it is perpendicular to this axis, in which case $Q_1 = 0$ and $Q_2 = (3/2)Q_0$.[35] Therefore for 3d→2p radiation

$$-0.32 \leq P \leq 0.48 \tag{46}$$

The resulting uncertainty in Q_{3d} is then + 11 percent, - 16 percent.

Systematic Error Due to Cascade

Hydrogen atoms formed in higher levels than the n=3 can decay spontaneously into the n=3 level and subsequently emit an H_α photon. It is not possible to determine precisely the effect of such transitions without measuring the cross sections for formation of many of the states having a higher energy than the n=3 state. However, a sufficiently accurate assessment of the possible error introduced by neglecting cascade can be made by noting the following facts. At the energies of the

present experiment, only the higher s states are formed in significant numbers, and the branching ratios for decay of these excited states favor a transition into the 2p state rather than the 3p. The cross sections for formation of these s states can be estimated with the aid of the rule given by Oppenheimer[29] that, at high energies, they vary with n as n^{-3}. Measurements by Hughes, et al.[31] near 100 keV tend to substantiate this prediction. Sample data were analyzed with appropriate allowance for cascade from the 4s state into the 3p state. The results showed only minor variations in the capture cross sections thus determined. The errors in cross sections introduced by neglecting cascade contributions from all states higher than n=3 are estimated to be no larger than those given in the following table.

Table 5. Uncertainty in the Capture Cross Sections Due to the Neglect of Cascade

	Helium Target	Nitrogen Target
In Q_{3s}	+ 0% - 3%	+ 0% - 3%
In Q_{3p}	±12%	± 8%
In Q_{3d}	± 6%	±10%
In Q_i	< 1%	< 1%

Systematic Error in Calibration of the Balmer Alpha Detector

Absolute calibration of the electron capture cross sections was accomplished as described on page 47 by comparison of H_α emission inten-

sities obtained from the charge transfer process with those obtained from the dissociative excitation of a molecular hydrogen target:

$$H^+ + H_2 \rightarrow H^+ + H^*(n=3) + H \qquad (47)$$

The absolute cross section for emission of the H_α line in this reaction was measured previously[23] in this laboratory by comparison with a tungsten filament standard lamp and was used as a convenient transfer standard. This emission cross section had been measured with an estimated uncertainty of ± 40 percent, and the accuracy of the calibration of the present cross sections is estimated to be ± 50 percent.

Total Uncertainty in the Collisional Destruction Cross Sections

The uncertainties in ρ, v, the effective decay length, variations in sensitivity over the face of the photomultiplier, and the neglect of cascade combine to produce a total systematic uncertainty in Q_i of about seven percent. Since these possible errors are independent of the random errors, the two may be combined as orthogonal vectors.[37] Since the random uncertainties are several times larger than those due to possible systematic errors, the total uncertainties are approximately equal to those given in Table 1.

Total Uncertainty in the Electron Capture Cross Sections

Ignoring for the moment the uncertainty in the absolute calibration, the measurements of cross sections for electron capture into the 3s state are estimated to have a total uncertainty of ± 15 percent or less in almost all cases. The estimates are shown by the error bars in

in Figures 10 and 13 (see Chapter V). Uncertainties arising from independent sources have been added as orthogonal vectors[37] in arriving at these estimates. The largest single contribution to the indicated uncertainties was due to the uncertainty in Q_i.

To these uncertainties must be added the ± 50 percent uncertainty in the absolute calibration. This has been omitted from the figures for clarity since an error from this source cannot affect the energy dependence of the cross section but could only raise or lower all the points by equal distances on the figures.

Cross sections for capture into the 3d states are presented in a similar way, omitting the estimated uncertainty in calibration. This cross section is about two orders of magnitude smaller than the cross section for formation of the 3s state. Therefore only a few percent of the measured light intensity is due to transitions from the 3d state. Random variations in the data are typically one to two percent, sometimes larger. As a result, the random variations in the measured values are sometimes more than 100 percent of the mean, and it has been necessary to assign an uncertainty factor of 2.5 (+ 150 percent, - 60 percent) to these measurements.

Random variations in the measurements of the cross section for capture into the 3p state are even larger than for the 3d state. The reason again is that only one or two percent of the Balmer alpha emission is due to radiation from atoms in the 3p state. The cross section for formation of this state is about an order of magnitude smaller than the cross section for formation of the 3s state, and less than 12 percent

of the 3p atoms decay by emission of an H_α photon. The remainder decay by Lyman beta. Because of large random variations in the measurements of the 3p cross sections, no error limits have been assigned. However, the measured values do allow the establishment of an upper bound for the cross section.

CHAPTER V

MEASURED VALUES OF THE CROSS SECTIONS

Measurements of the cross section for the formation of the excited states of atomic hydrogen are shown in Figures 10 through 15 for targets of He and N_2. Uncertainty in the absolute values of cross sections is estimated to be ± 50 percent, most of which comes from uncertainty in the emission cross section data to which the present work was normalized. Uncertainty in the relative variations of cross sections with energy are indicated with error bars in Figures 10, 11, 13, and 14. A full discussion of error limits is given in Chapter IV.

Figure 10 shows the cross section for the formation of the 3s state for protons incident on helium. For comparison, the predictions by Mapleton and the previous measurements by Hughes, et al.[10] and by Andreev, et al.[11] are also shown. The general form of our measurements is in agreement with Mapleton's predictions.[2] The systematic discrepancy between theory and experiment might be due to an erroneous calibration of detection sensitivity. It appears that the present measurements confirm the general validity of Mapleton's theory down to impact energies of 75 keV.

Figure 11 presents measurements of the cross section for the formation of the 3d state in a helium target, again compared with predictions of Mapleton.[2] This cross section is about two orders of magnitude smaller than the cross section for the formation of the 3s state,

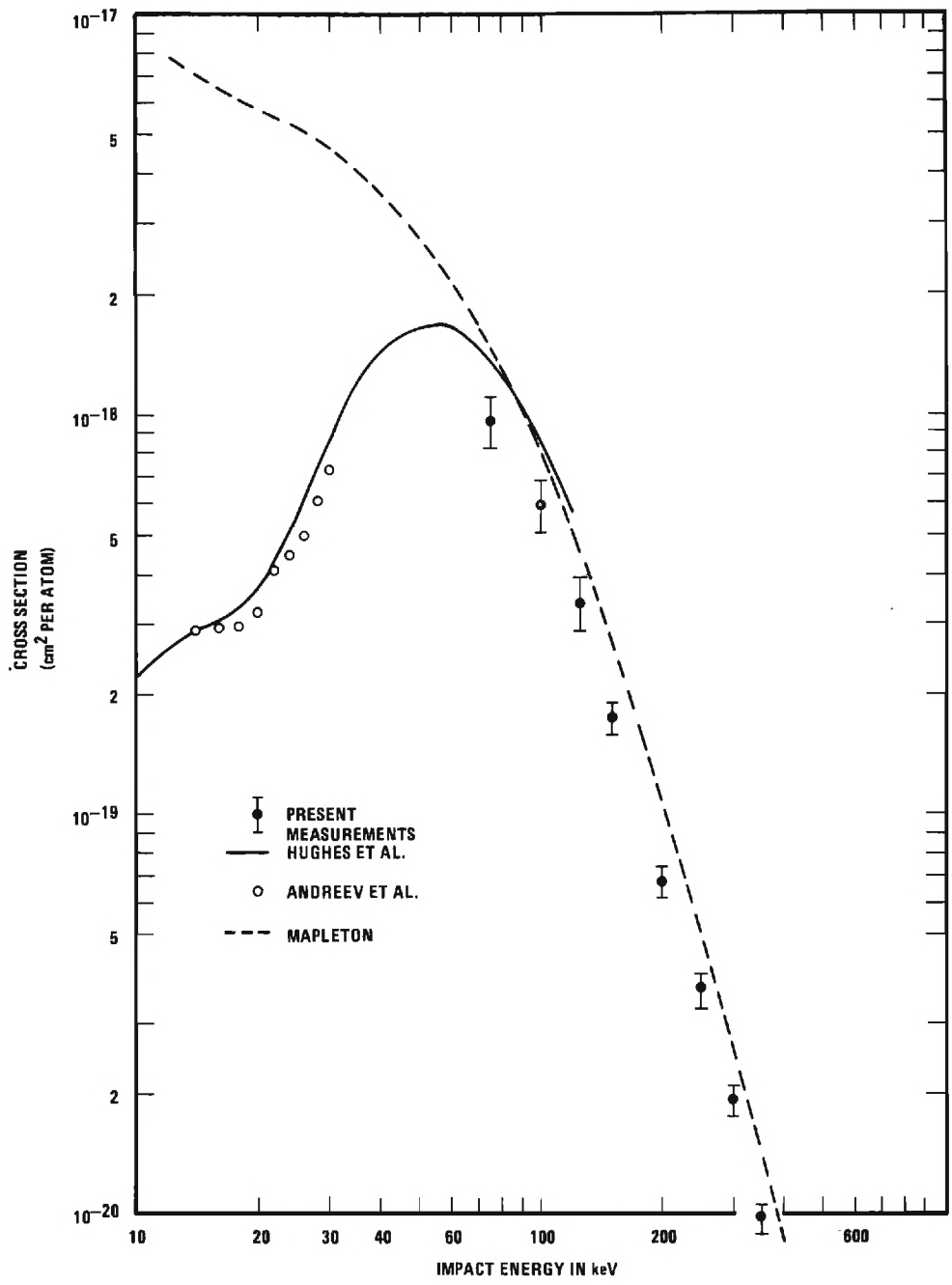

Figure 10. Cross Section for the Formation of H(3s) Atoms in Helium. (The process is represented by the equation $H^+ + He \rightarrow H(3s) + He^+$. Present measurements are shown along with those made by Hughes et al.[10] and by Andreev et al.[11] Also shown are predictions of the Born approximation calculated by Mapleton[2] using the post-collision potential for the process $H^+ + He(1s^2) \rightarrow H(3s) + He^+(1s)$.)

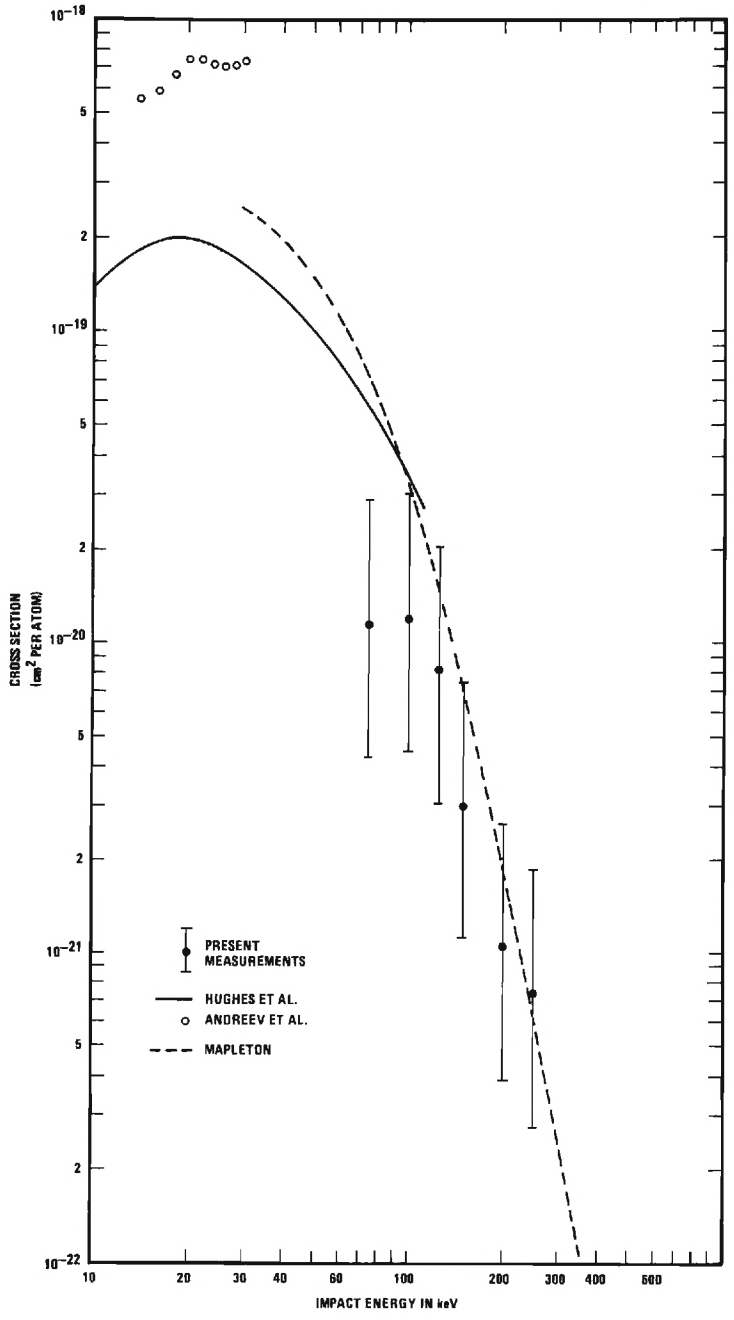

Figure 11. Cross Section for the Formation of H(3d) Atoms in Helium. (The process is represented by the equation $H^+ + He \rightarrow H(3d) + He^+$. Present measurements are shown along with those made by Hughes et al.[10] and by Andreev et al.[11] Also shown are predictions of the Born approximation calculated by Mapleton[2] using the post-collision potential for the process $H^+ + He(1s^2) \rightarrow H(3d) + He^+(1s)$.)

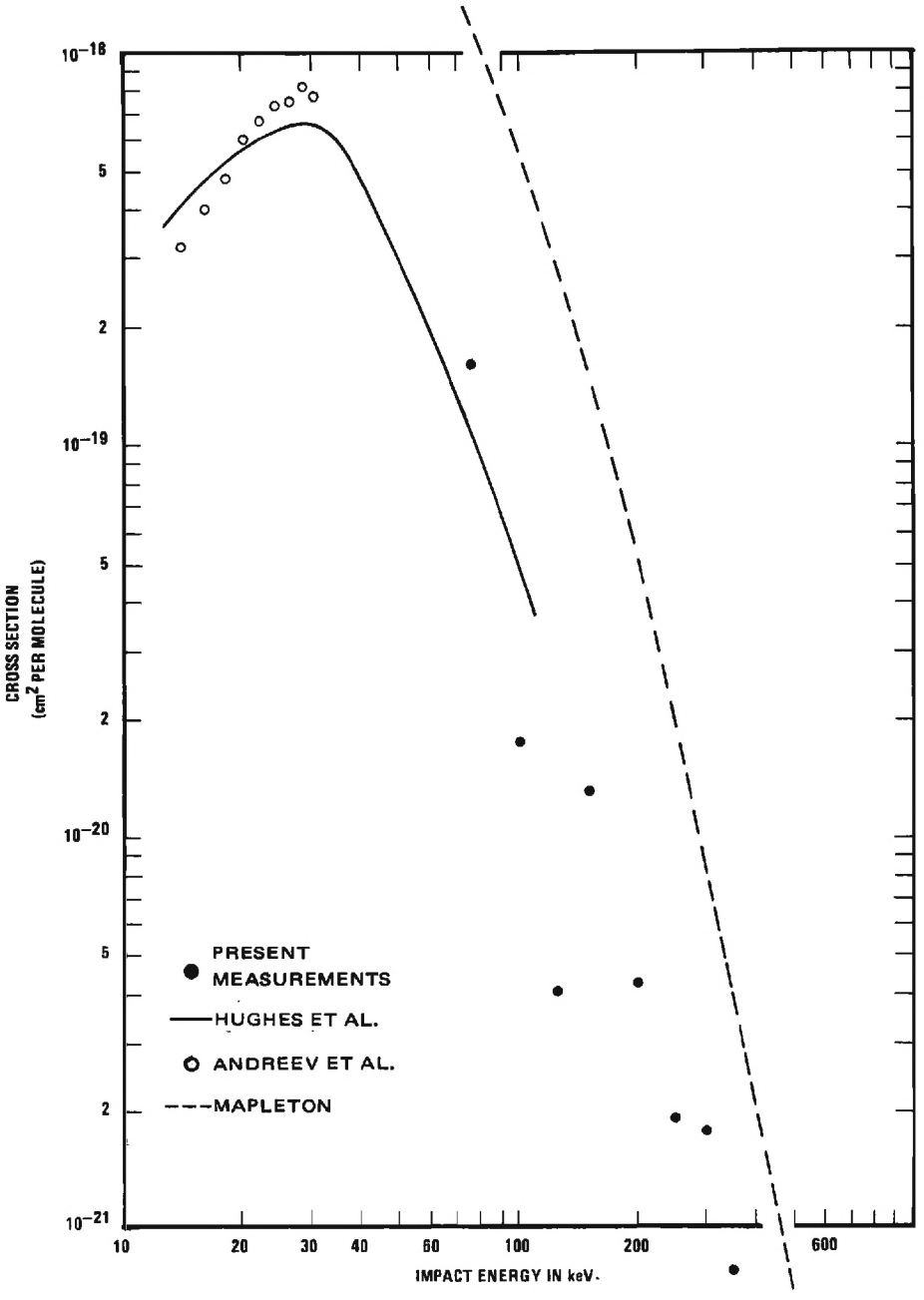

Figure 12. Cross Section for the Formation of H(3p) Atoms in Helium. (The process is represented by the equation $H^+ + He \rightarrow H(3p) + He^+$. Present measurements are shown along with those made by Hughes et al.[10] and by Andreev et al.[11] Also shown are predictions of the Born approximation calculated by Mapleton[2] using the post-collision potential for the process $H^+ + He(1s^2) \rightarrow H(3p) + He^+(1s)$.)

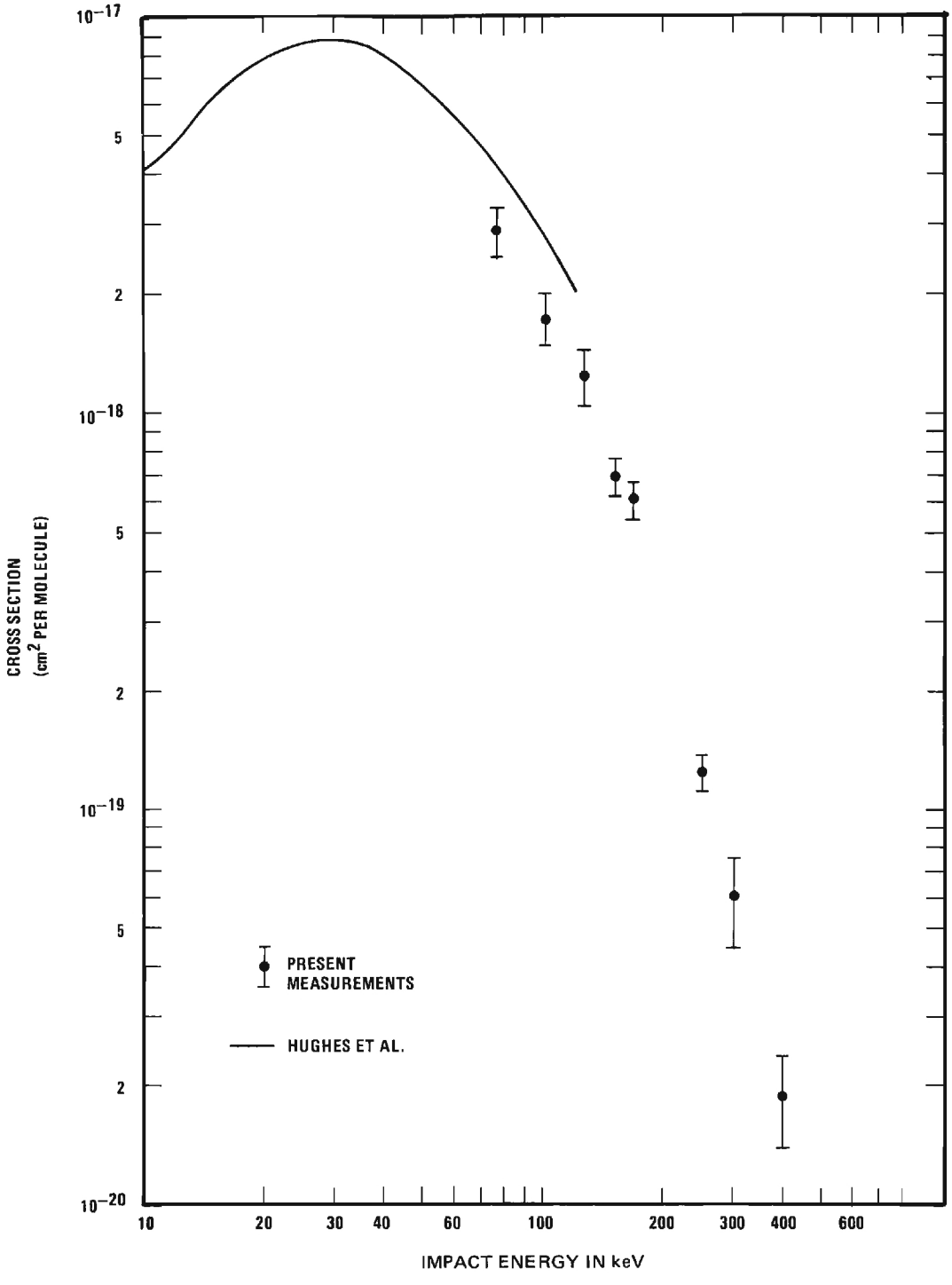

Figure 13. Cross Section for the Formation of H(3s) Atoms in Nitrogen. (The process is represented by the equation $H^+ + N_2 \rightarrow H(3s) + N_2^+$. Present measurements are shown along with those made by Hughes et al.[10])

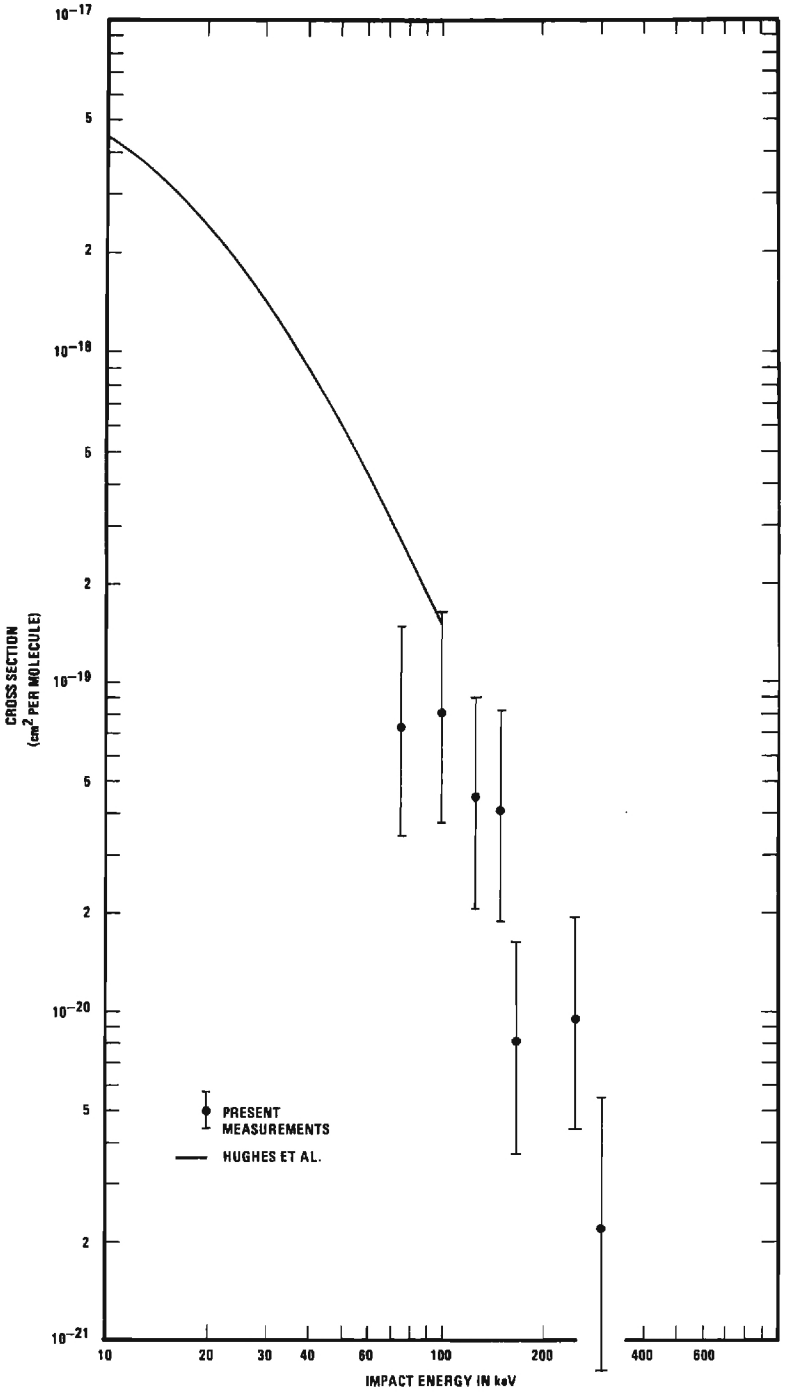

Figure 14. Cross Section for the Formation of H(3d) Atoms in Nitrogen. (The process is represented by the equation $H^+ + N_2 \rightarrow H(3d) + N_2^+$. Present measurements are shown along with those made by Hughes et al.[10])

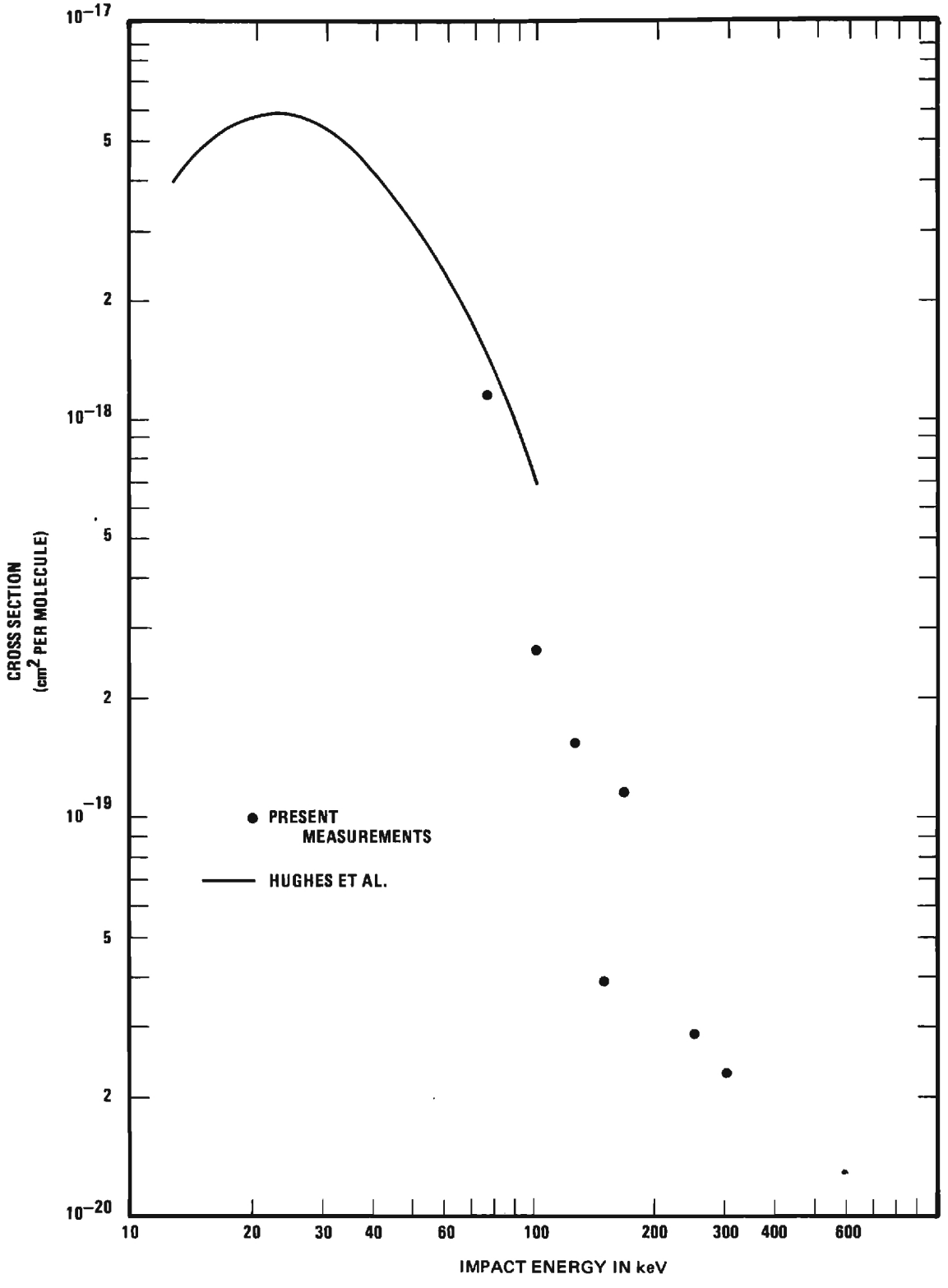

Figure 15. Cross Section for the Formation of H(3p) Atoms in Nitrogen. (The process is represented by the equation $H^+ + N_2 \rightarrow H(3p) + N_2^+$. Present measurements are shown along with those made by Hughes et al.[10])

which means that only a few percent of the measured light intensity is due to transitions from the 3d state. Statistical fluctuations in the data are typically one or two percent, sometimes larger. As a result it has been necessary to assign very large random error bars to the data for this state. Nevertheless the agreement between theory and experiment is surprisingly good.

The measurements of the cross sections for the formation of the 3p state (Figure 12) are so poor that it would be misleading to assign error bars. Generally speaking, they do compare with the measurements by Hughes, et al.[10] and allow us to establish an upper bound to the cross section for the formation of the state. This bound lies below the theoretical predictions of Mapleton[2] by a factor of between four and ten at all energies from 75 to 400 keV. This very large discrepancy is most surprising. There seems no obvious reason why theoretical predictions should be good for the 3s and 3d states while being very poor for the 3p level. More recently the cross section for the 3p state has been determined utilizing the gas cell configuration of the experiment. This new procedure provides a much better measurement of the short-lived states than was obtainable with the present scheme. The new data are in general agreement with those presented here; the 3p state cross section again lies far lower in magnitude than theory predicts. There are also general theories for the prediction of relative populations of excited states from the work of Hiskes,[38,39,40] and of Butler and May.[41] These theories are in general agreement with the work by Mapleton[2] and therefore in disagreement with the present experiment. It must be concluded that the existing theory is in error.

Figures 13, 14, and 15 show the cross sections for formation of the 3s, 3d, and 3p states of H by impact of H^+ on a target of N_2. Their magnitudes are several times larger than for a helium target, but the energy dependences are similar. There are no detailed theoretical predictions with which these may be compared.

Figures 16 and 17 show the cross sections for the destruction of the 3s excited state by impact on targets of helium and nitrogen, respectively. Comparisons are made with Bates and Walker's theoretical predictions of the cross sections for ionization of this state.[1] In the case of a nitrogen target, the magnitude of the present measurements appears to be in agreement with these predictions within experimental uncertainty, although a somewhat different energy dependence is indicated. For a target of helium, the magnitudes of the predictions and the measurements differ by a little more than the estimated experimental uncertainties, but in no case more than a factor of two. However, the energy dependences are substantially different.

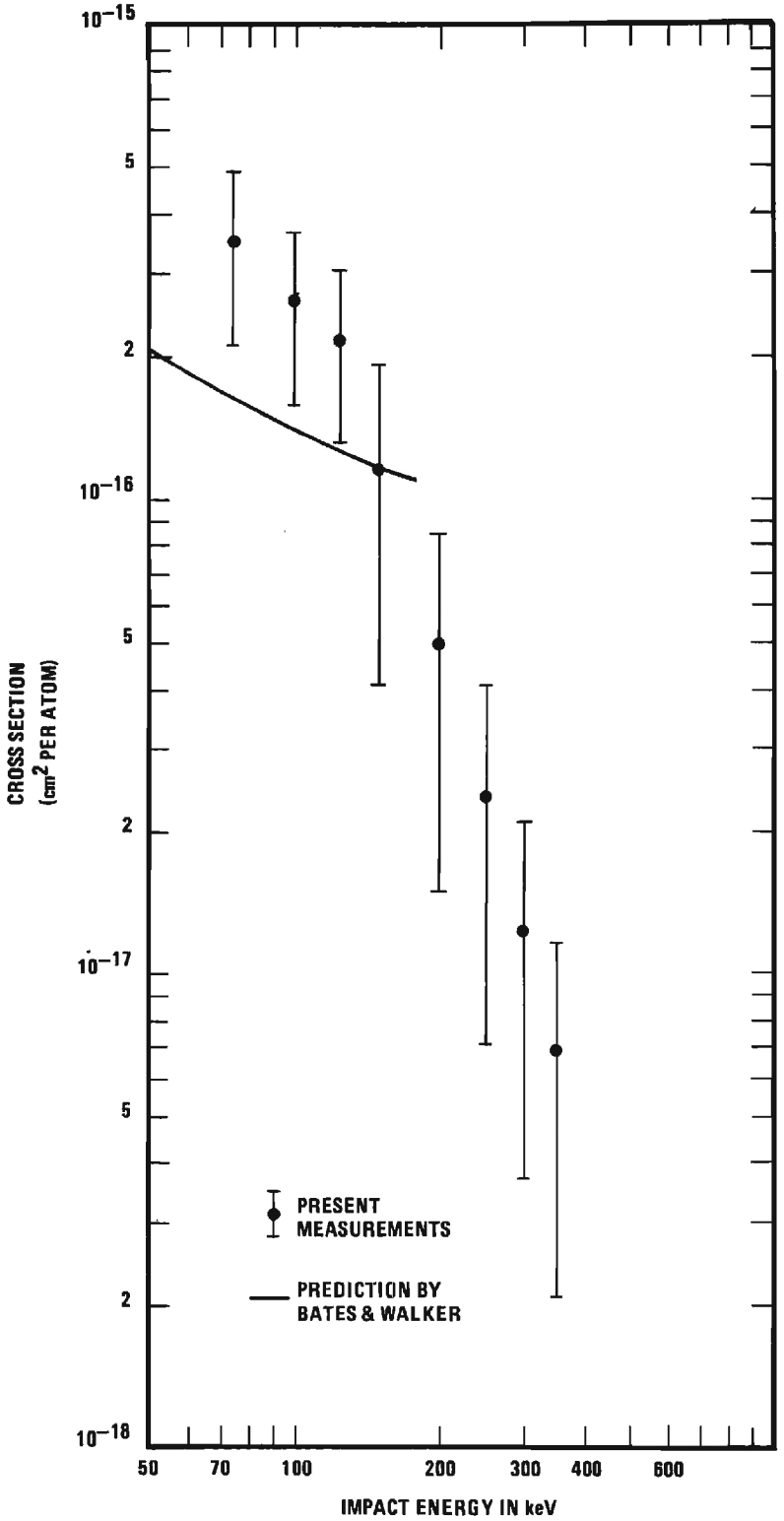

Figure 16. Cross Section for the Collisional Destruction of H(3s) Atoms by Impact on Helium. (Present measurements are shown along with predictions by Bates and Walker[1] for the ionization of H(3s) atoms by impact on helium.)

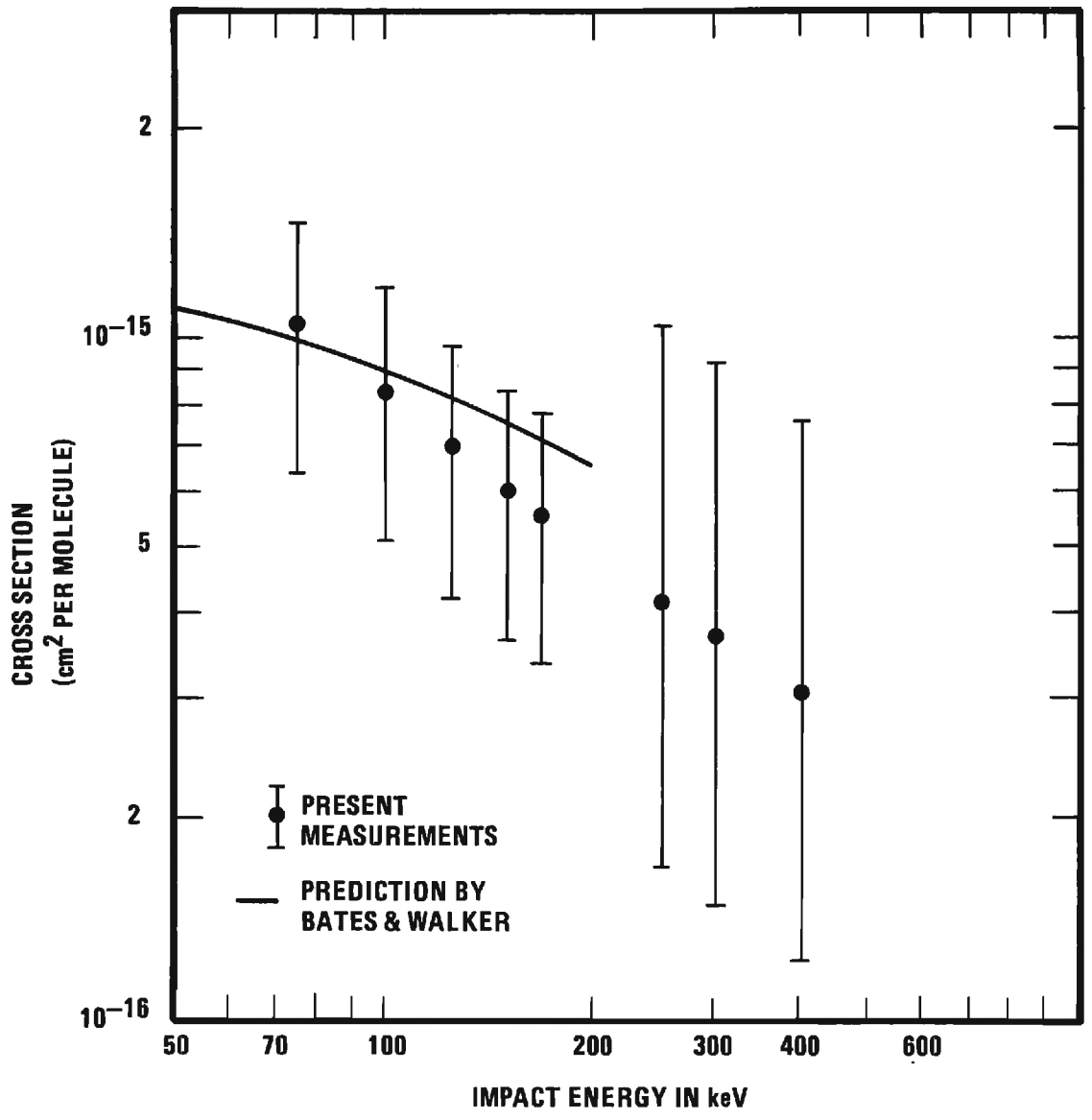

Figure 17. Cross Section for the Collisional Destruction of H(3s) Atoms by Impact on Nitrogen. (Present measurements are shown along with predictions by Bates and Walker[1] for the ionization of H(3s) atoms by impact on nitrogen.)

CHAPTER VI

COMPARISON WITH OTHER WORK

The results of the present experiment will be compared with theory in order to gain some insight into the validity of the approximations made in theoretical calculations. It is also possible to correlate the present results with the experimental data of other research groups obtained at lower impact energies.

Comparison with Calculations of Electron Capture Cross Sections

The capture cross sections measured in the present experiment may be compared directly with the values predicted by the Born approximation for capture into the 3s, 3p, and 3d states and with a prediction of the ratio of these cross sections. Further insight into the relationship between theory and experiment may be obtained by a consideration of coupled state calculations which are available for the 2s and 2p states. It is also of interest to consider theoretical calculations for capture from a one-electron atom in order to ascertain whether there is any correspondence between the results of such a theory and experimental results for targets of He and N_2.

Calculations for a Target of Helium

The theoretical work most directly applicable to the present measurements of charge transfer cross sections is that of Mapleton.[2] He has utilized Born's approximation to calculate cross sections for the processes

$$H^+ + He(1s^2) \rightarrow H^*(3s,\ 3p,\ \text{or}\ 3d) + He^+(1s) \qquad (48)$$

for impact energies from 7 to 1000 keV. The experiment measured the cross section for the sum of all possible final states of the He^+ ion, but from Mapleton's predictions it is estimated that at least 90 percent of such collisions leave the ion in the 1s state. Mapleton has made calculations for both prior- and post-collision potentials. If exact atomic wave functions were known for the helium atom, as they are for hydrogen, the two sets of calculations would yield identical results. The exact atomic wave functions for the helium atom are not known and the wave function used by Mapleton

$$\frac{Z^3}{\pi\, a_o{}^3} \exp\left[-\left(\frac{Z}{a_o}\right)(r_1 + r_2)\right], \qquad (Z = 1.6875) \tag{49}$$

is admittedly rather crude. However, this wave function yields prior and post total capture cross sections which are within 20 percent of one another and are in fair agreement with experimental measurements. According to Mapleton,

> the reason for this apparent success appears to emerge from the good representation for the wave function for helium over the region of configuration space that provides the major contribution to the cross section for ... [capture into the ground state of H] ... which process provides the major contribution to the total capture cross section. On the basis of this close agreement, it is reasonable to expect that the exact Born cross sections would not differ radically from these approximate values.[2]

Cross sections for electron capture into the ground state have been calculated by Bransden and Sin Fai Lam,[19] using the impact parameter formulation, for a number of approximate helium wave functions including the one used by Mapleton. They conclude that the calculated cross sections are not very sensitive to the helium wave function employed,

for proton energies between 30 keV and 10 MeV.

Mapleton's prediction of the cross section for electron capture into the 3s state has approximately the same energy dependence as the present measurements but appears to be about 50 percent higher in magnitude (Figure 10). This systematic discrepancy lies just within the estimate of experimental uncertainty and could be due to an error in calibration of the detection sensitivity. The measurements apparently confirm the general validity of Mapleton's theory for impact energies from 75 to 400 keV.

Because of the small magnitude of the cross section for capture into the 3d state, the experimental uncertainties in its measurements are considerably larger than those for the 3s state. However, the same systematic discrepancy of about 50 percent exists between these measurements and Mapleton's predictions of the 3d cross section. Otherwise the agreement seems remarkably good.

The measurements of the cross section for formation of the 3p state are admittedly very poor. They do, however, allow the establishment of an upper bound to the cross section. This bound lies below Mapleton's predictions by a factor between four and ten at all energies from 75 to 400 keV. This large discrepancy is quite surprising, and there seems no obvious reason why theoretical predictions should be good for 3s and 3d states but poor for the 3p state. Recently the cross section for the 3p state has been measured utilizing the alternative configuration of the experimental apparatus described on page 11. This procedure provides a much better measurement of the short-lived states than was obtainable with the previous scheme. The new data are in general

agreement with the work presented in this thesis confirming that the 3p cross section lies far lower in magnitude than Mapleton's theory predicts. The conclusion is that the theory is in error for this case.

The explanation may be in the crudeness of the helium wave function used by Mapleton. It is conceivable that, although it is a good representation over the region of configuration space providing major contributions to cross sections for charge transfer into the 1s, 3s, and 3d states, it may be less accurate in the region of configuration space important to the 3p cross section.

In a subsequent paper,[18] Mapleton has used the six-parameter helium wave function of Hylleras to calculate Born prior and post cross sections for the process

$$H^+ + He(1s^2) \rightarrow H(1s) + He^+(1s) \qquad (50)$$

that is, capture into the ground state. The discrepancy between the results using prior- and post-collision potentials is thereby reduced from 20 percent to less than one percent, indicating that the wave function is adequate for this type of scattering calculation.

The newer values of 1s capture cross section[18] are in better agreement with his earlier 1s predictions based on the post-collision potential than with those based on the prior potential.[2] For this reason, comparisons in this thesis with Mapleton's predictions[2] are based on his post-collision results. Unfortunately, calculations for capture into the n=3 state were not done using the Hylleras wave function.

It is possible that this wave function would also give a smaller

3p cross section, in better agreement with the measurements, but that is purely speculation.

Calculations have been made by Hiskes[39,40] of the ratios $Q_{3s}:Q_{3p}:Q_{3d}$ for protons incident on helium. A simplified form of the Brinkman-Kramers matrix element was employed, and Hartree-Fock wave functions were employed for the target atom. Within the energy range of this experiment, ratios obtained[40] in this way agree well with those obtained from Mapleton's predictions,[2] and are therefore in disagreement with the present experimental measurements. At energies of 10 and 30 keV, the results of Mapleton,[2] and Hiskes[39] are in disagreement, indicating that the different theories diverge at lower energies. However, in this energy range the Born approximation, which Mapleton employs, may not be valid.

The impact-parameter formulation has been used by Sin Fai Lam[42] to calculate cross sections for the electron capture reactions

$$H^+ + He(1s^2) \rightarrow H(1s,\ 2s,\ 2p) + He^+(1s)$$

over the energy range one to 1000 keV. The calculation was performed with allowance for coupling among these states during the collision process. Mathematically, this means that the time-dependent wave function describing the active electron during the collision is approximated by a linear combination of the initial state function and the wave functions of all the given final states. The coefficients in this linear combination are time-dependent, and the capture cross sections are easily obtained from their values at an infinite time after the collision.

Simpler approaches consider only one possible final state and utilize a wave function during collision which is a linear combination of only this state and the initial state. Since, in principle, a complete set of functions is needed to describe the electron during collision, the inclusion of more state functions should produce a more accurate prediction, particularly if the choice of included functions is cleverly made.

Sin Fai Lam's predictions of the cross sections for capture into the 2s and 2p states have been scaled by the n^{-3} rule[29,30] to produce estimates of the 3s and 3p cross sections. A comparison shows that, for the energy range of the present experiment, the scaled cross section lies higher than Mapleton's prediction[2] of the 3s cross section by an amount which increases with energy from about 10 percent at 100 keV to about 90 percent at 400 keV. Since Mapleton's calculations are already larger than the present measurements, these scalings of Sin Fai Lam's s state predictions agree less well with this experiment than do Mapleton's, and energy dependence is significantly different from that indicated by the present measurements.

However, the scaling of Sin Fai Lam's 2p prediction produces an estimate of the 3p cross section about a factor of two smaller than Mapleton's, and therefore in somewhat better agreement with estimates of the 3p cross section obtained from the present experiment. The allowance in the calculation for coupling to the 1s and 2s states is likely to have been responsible for the improvement in this prediction over Mapleton's.

Although the comparison of present measurements with Sin Fai Lam's calculations shows a substantial discrepancy in magnitude for both the s and the p cross sections, the ratio of his predicted cross sections is clearly much nearer the experimental results than the prediction of this ratio by Mapleton and by Hiskes.

In conclusion, there is general agreement of the energy dependence of the data for formation of the 3s state with the predictions of Mapleton.[2] There is little correspondence between the predictions of the 3p cross section and experiment. It would appear that further work to include coupling to yet other competing processes, as suggested by Bransden and Sin Fai Lam,[19,42] might further elucidate this problem.

Calculations for a Target of Atomic Hydrogen

Predictions for the reaction

$$H^+ + H(1s) \rightarrow H^* + H^+ \qquad (51)$$

are more amenable to calculation than those for any other target since exact wave functions are known for all participants in the collision. The resulting cross sections might be expected to give some indication of the form of the cross sections for electron capture for other targets.

Calculations by Bates and Dalgarno,[4] Mapleton,[43] Jackson and Schiff,[3] and May[30‡] indicate that the ratio $Q_{3p}/(Q_{3s} + Q_{3p} + Q_{3d})$ ranges from 40 percent to 50 percent at 75 keV down to 12 percent to 22 percent at 400 keV, again much larger values than are indicated by the present

---

‡Calculations in reference 30 are done in the limit of large n, but the ratios quoted do not differ significantly from those calculated by Bates and Dalgarno[4] and by Mapleton[43] for n=3.

measurements for targets of helium and molecular nitrogen. May[30] presents only the ratios of cross sections, but the 3s cross sections presented in the other three references[3,4,43] are scattered within a factor of four of the measured cross section for a target of helium at 75 keV. However, the predicted cross sections for atomic H decrease much more rapidly with increasing energy than the measured values for helium. There appears to be little correspondence between the predictions for a target of atomic H and the present measurements for targets of He and N_2.

Comparison with Other Experimental Measurements

Measurements of the cross sections for electron capture into the n=3 states have been made by Hughes, et al.[8,9,10] at energies from five to 115 keV, for several target gases including He and N_2 and by Andreev, et al.[11] at energies from 14 to 30 keV for three noble gases including He. Their results are shown in Figures 10 through 15 along with results of the present experiment and Mapleton's predictions.[2] Measurements have also been made by Berkner, et al.[44] of the cross section for electron capture into the n=6 level of hydrogen by five to 70 keV protons in neon and magnesium vapor. Their technique is in some ways similar to that of the present experiment. It is shown, however, that assumptions made in their analysis of data are unsubstantiated and perhaps inconsistent with the results of the present experiment.

Measurements of Cross Sections for Capture into the n=3 Level

The experimental system employed by Hughes and his co-workers is essentially the scheme described as an alternative to that used for the present measurements (see Chapter II). A gas cell in which the colli-

sions occur is followed by an evacuated flight tube along which the H_α intensity is measured as a function of distance from the exit of the gas cell.

As shown in the figures, the energy range of the present measurements overlaps that of Hughes' measurements. Measurements of emission cross sections reported by Hughes' group have been consistently larger in magnitude than those reported by this laboratory[23,45,46] due to differences in calibration of the two experimental systems. The present case is no exception; where the energy ranges overlap, Hughes' values for Q_{3s} for He and N_2 are about 40 to 50 percent larger than those measured in the present experiment, a discrepancy which is within experimental uncertainties.

A comparison with Hughes' measurements[10] of the cross section for capture into the 3d state with either target (Figures 11 and 14) would suggest a discrepancy similar to that observed in the measurements of Q_{3s}.

Little can be said about the comparison of the present measurements of the 3p cross section with Hughes'[10] except that there is no evidence of a major disagreement.

Collisional destruction of excited atoms appears to have been insignificant for Hughes' experiments. His paper states[8] that observed emission intensities were proportional to target gas densities. This observation is not in contradiction with results of the present experiment since, for the target pressures utilized, the length of his collision cell was substantially less than the mean free path for electron loss.

In summary, where a direct comparison with measurements by Hughes is possible, his cross sections for electron capture appear to be about 40 to 50 percent larger than the present measurements due to a discrepancy in absolute calibration of detection efficiency. Even so, the two sets of measurements are within the combined experimental uncertainties and are considered to be in agreement.

The cross sections for electron capture into the n=3 states from a helium target have been measured by Andreev, et al.[11] in the energy range 14 to 30 keV by a method which differs fundamentally from those utilized in the present experiment and by Hughes.[10] The scheme requires measurements of emission intensities of Balmer alpha and Lyman beta photons in the presence and in the absence of an external electric field. The assumption is made that the total cross section for the "excitation" (Andreev's word) of the n=3 level is independent of the electric field. Relations between the measured cross sections are then used to deduce Q_{3s}, Q_{3p}, and Q_{3d}. There is some question as to the validity of the basic assumption that the total excitation cross section of the n=3 level is independent of the externally applied field.

The measurements are presented in Figures 10, 11, and 12. Andreev's measurements of Q_{3s} appear on the average to be about 15 percent smaller than Hughes' but are in fair agreement. His measurements of Q_{3p} are also in fair agreement with Hughes' as to magnitude (Figure 12) although the energy dependences are not the same. Andreev's measurements of this particular cross section are not subject to the question raised by his assumption of independence of n=3 cross section and applied

field. The 3p measurement was performed simply by measuring the Lyman beta intensity, which is due entirely to emission from 3p atoms. His measurements of Q_{3d} are larger than Hughes' by a factor of three to four and further doubt is therefore cast upon the validity of his basic assumption. His total cross section for excitation of the n=3 level ($Q_{3s} + Q_{3p} + Q_{3d}$) is about 30 percent larger than Hughes' because of this discrepancy in the 3d measurements.

Other Measurements of Electron Capture Cross Sections

Although no direct comparison is possible with the measurements by Berkner, et al.[44] for capture into the n=6 level from targets of Mg vapor and neon, a discussion of their method and results may be of value. In their arrangement, a collimated, momentum-analyzed beam of H^+ or D^+ passed through an oven in which Mg granules could be heated to produce magnesium vapor or, with the heater switched off, neon could be introduced as the target. Impact energies ranged from five to 70 keV. After charge exchange collisions in the oven, the beam contained H^+, H^-, and H atoms in various states. Radiation from the decay of excited atoms in the beam was observed at a single location just beyond the exit aperture of the oven. The emission was analyzed for the Balmer delta component (n=6 → n=2, 4102 Å) and detected by a photomultiplier. Detection efficiency was measured by comparison with the emission from the 0-0 first negative band of N_2^+ (3914 Å) produced by bombardment of N_2 by 60 keV protons and normalized to a weighted average of cross sections published by other experimenters. The assumption was made that the detection efficiencies at 3914 Å and at 4102 Å were approximately equal.

Instead of attempting the admittedly difficult task of identifying the contributions of the three separate angular momentum substates to the H_δ emission, the data were analyzed under the assumption that the population of the n=6 level at the exit aperture of the oven was distributed statistically over the possible substates. There is no evidence to indicate that the n=6 level is initially populated with such a distribution. Theoretically predicted cross sections indicate that most of the electron capture into the n=6 level takes place into the s, p, or d states with essentially none into the f, g, or h states, although the latter trio includes 27 of the 36 available substates. The present experiment and others[8,9,10,31] which have measured populations of the n=3 and n=4 substates have, in fact, shown that the populations have an entirely different distribution, leaning heavily toward the state having the smallest statistical weight, the s state. However, the substates of the n=6 level are less widely separated in energy than those of the lower levels and are therefore more readily mixed. Stark perturbations due to stray fields in the apparatus and to motion across the earth's magnetic field are likely to cause mixing of substates of this level, and it is conceivable that the population tends toward a statistical distribution. No evidence is presented to substantiate the assumption, which is basic to the analysis of the data, and the authors themselves indicate that they harbor some reservations concerning its validity.

The presentation of most of the data is based on the specific assumption (which we call here assumption (1)) that the substates are

shuffled into statistical equilibrium before leaving the oven, but that beyond its exit aperture, no more shuffling occurs and field-free lifetimes apply. However, data are also presented for several alternative models:

(2) a statistical distribution achieved in the collisional formation process with no subsequent shuffling,

(3) a statistical distribution achieved and maintained by shuffling both inside and beyond the oven,

(4) a distribution into only s, p, and d substates according to Born calculations with no subsequent shuffling,

(5) formation only of s states with no subsequent shuffling,

(6) formation only of p states with no subsequent shuffling,

(7) formation only of d states with no subsequent shuffling.

Each of the seven cases is worked out both with field-free lifetimes and again with Stark lifetimes. Cross sections obtained from the data on the basis of assumptions (1), (2), and (3) with either Stark or field-free lifetimes all lie within 25 percent of one another. The use of assumption (4) reduces the cross sections by a factor of two to three from those presented using assumption (1). The use of assumptions (5), (6), or (7) causes more drastic changes in the results, but the assumptions seem rather implausible.

Unless the assumed shuffling is complete, the population distribution will depend on the beam energy because the fraction of the n=6 atoms originally formed in a given substate will in general vary with energy. Born calculations quoted by Berkner predict such a variation. Because of this possibility, there is doubt as to the energy dependence

of the cross sections presented.

The absolute calibration of the photon detector was based on the assumption that its efficiency was the same for the emission band of nitrogen at 3914 Å as for the H_δ line at 4102 Å. Because the nitrogen line is spread by the rotational structure over tens of Angstroms, all of which should be detected, whereas the H_δ emission is contained within a small fraction of an Angstrom, and because the two sets of emissions are separated by nearly 200 Å, the assumption is somewhat questionable.

There are serious questions, then, with regard to both the magnitude and the energy dependence of the cross section values presented, and it is suggested that these values be considered as no more than an indication of the order of magnitude.

Other experimenters have measured cross sections for electron capture by protons into various orbits, but most of the work concerning excited states has been done for capture into the 2s and 2p states at considerably lower impact energies than those used in the present experiment.

Dahlberg, et al.[48] have measured a relative cross section for Lyman alpha emission (2p→1s) resulting from the impact of protons on a nitrogen target over the energy range 20 to 130 keV.

$$H^+ + N_2 \rightarrow H(2p) + [N_2^+] \qquad (52)$$

Since the Lyman alpha line is due to a single transition, 2p→1s, there is no problem of separating transitions. However, the author states that a pure proton beam could not be obtained at the entrance to the

target cell due to high background pressure in a preceding cell which was used in another experiment for the production of a neutral beam. The Lyman alpha emission cross section was also reported[48] for H(1s) impact and was larger than the cross section for emission by process (52) throughout the energy range. The ratio of the two cross sections increased from about 1.3 at 20 keV to about 10 at 130 keV. This suggests the possibility of a substantial energy-dependent uncertainty in the cross section measurement for H^+ impact, even if a correction was made for the emission due to the neutral component of the beam.

No corrections were made for the effects of cascade. The effect of the finite lifetime of the 2p state was also ignored, but the resulting error was estimated to be less than 20 percent. This error tends to increase with increasing energy. The possibility of Doppler effects was not mentioned in the report,[48] but it appears from the description of the apparatus that errors from this source may have been small.

Because of the several possibilities for significant energy-dependent systematic error, it is risky to make any comparisons with the results of the present experiment.

Other measurements pertaining to the capture of electrons into excited states by protons are listed in Table 6.

Table 6. Measurements Pertaining to the Capture of Electrons into Excited States by Protons

Reference	Energy Range (keV)	Target Gases	States or Emission Line
Colli, et al.[49]	7 - 40	He, H_2	2s
Jaecks, et al.[50]	1.5 - 23	He, Ne, Xe, Ar	2s
Dose[51]	3 - 71	He	2s, 2p
Andreev, et al.[52]	10 - 40	He, Ne, Ar, Kr, Xe	2s, 2p
Ryding, et al.[53]	40 - 200	H_2, H, He	2s
Hughes, et al.[8]	5 - 115	He, Ar, Ne, N_2, H_2, O_2	3s
Andreev, et al.[11]	14 - 30 10 - 30	He Ar, Ne	3s, 3p, 3d 3s, 3p, 3d
Hughes, et al.[31]	5 - 120	He, Ar, Ne, N_2, H_2, O_2	4s
DeHeer, et al.[54]	5 - 35	H_2, He, Ne, Kr	2p, 3p
Pretzer, et al.[55]	1 - 25	He, Ne, Ar, Xe, Kr	2p
Gaily, et al.[56]	0.5 - 15	He, Ne, Ar	2p and its magnetic substates
Andreev, et al.[57]	10 - 40	He, Ne, Ar, Kr, Xe	Lyman beta, 3p
Bayfield[58]	2 - 70	H_2, Ar	2s
Teubner, et al.[59]	0.4 - 26	Ar, Ne, He	Lyman alpha (polarization fraction only)

Table 6. Measurements Pertaining to the Capture of Electrons into Excited States by Protons (Concluded)

Reference	Energy Range (keV)	Target Gases	States or Emission Line
Sellin[60]	5 - 20	H_2	2s
Andreev, et al.[61]	10 - 35	H_2	2s, 2p, Lyman beta, 3p
Hughes, et al.[9]	10 - 35	N_2	3s, 3p, 3d
Dahlberg, et al.[48]	10 - 130	N_2	2p
Sellin and Granoff[62]	2 - 30	K, Cs, Rb vapors	2s
Donnally, et al.[63]	0.16 - 3	Cs vapor	2s
Cesati, et al.[64]	8 - 40	H_2	2s
Dahlberg, et al.[65]	20 - 130	H_2	Lyman alpha
Hughes, et al.[10]	10 - 120	He, Ar, Ne, N_2, H_2, O_2	3s, 3p, 3d
Berkner, et al.[44]	5 - 70	Mg vapor, Ne	n=6 level

Comparison of the Collisional Destruction Cross Section with Predictions

The cross sections for collisional destruction of H(3s) atoms have been measured in the present research by the method described in Chapter III. Bates and Walker[1] have calculated cross sections for the quenching of the emission from this state and it is interesting to make a comparison. Their calculation is done with the aid of the classical impulse approximation, and a simple formula is derived which expresses the cross section as the product of the (measured) total free electron scattering cross section (for the same velocity as the impact velocity of the atoms) and a "correction" factor. For $n \geq 3$ and for velocities in the range used in this experiment, the "correction" factor is essentially unity, implying that almost all encounters result in the ionization of the hydrogen atom. Both Lodge[47] and Butler and May[41] make a similar implication. Bates and Walker[1] state that "encounters which merely cause a change in the azimuthal quantum number must therefore be relatively rare; and contrary to the assumption in some of the earlier investigations of auroras they cannot bring the population distribution amongst the states of a level into statistical equilibrium." They further state that "the effect of the orbital velocity is so small for the excited states of interest that negligible error is introduced by taking the loss cross sections, Q_n, from level n to apply to the separate $n\ell$ states." They also point out that most experimental studies of hydrogen line emission from H or H^+ beams passing through atmospheric gases have been done at molecular number densities which were high enough

for quenching to be significant. Some of the experimenters

> . . . found that the intensity of the emission was proportional to the density of the gas, which might at first be thought to be inconsistent with the occurrence of quenching. The explanation of the apparent anomaly is simply that the mean free path toward electron loss greatly exceeded the distance along the beam from the place where it entered the collision chamber to the region under observation.[1]

For the present experiment, the product of the collision chamber length and the target gas number density was sufficient that quenching was observable.

The method of determining Q_i, the cross section for destruction of the 3s state, in the present experiment required that an apparent lifetime or decay length be fitted to the data of emission intensity versus target penetration depth x for large x where 3p and 3d contributions to the H_α emission had reached their asymptotic levels (see pages 27, 52). Because the curvature of the single remaining exponential in this region was not great and because of statistical scatter in the data, the accuracy of the measurement of the apparent decay length $(1/v\tau_{3s} + \rho Q_i)^{-1}$ was not great. Uncertainty in the measurement of Q_i was further increased by the ratio of the quantity $(1/v\tau_{3s} + \rho Q_i)$ to ρQ_i.

For a target of nitrogen, at the highest target pressures utilized (0.6×10^{-3} Torr), ρQ_i was approximately equal to $1/v\tau_{3s}$ and the estimated uncertainty in Q_i was ± 40 percent. Within the experimental uncertainty, the magnitude of these measurements appears to be in agreement with Bates and Walker's predictions,[1] although a somewhat different energy dependence is indicated (Figure 17).

For a target of helium, Q_i is about five times smaller, and even though higher target pressures were used (up to 1.5×10^{-3} Torr), ρQ_i rarely exceeded half the value of $1/v\tau_{3S}$. The estimated uncertainty in Q_i therefore ranges upward from ± 40 percent at the lower energies, where signal levels were largest and statistical fluctuations smallest, to ± 70 percent at the higher energies. Within these rather large experimental uncertainties, the agreement with Bates and Walker's predictions is again satisfactory in magnitude although the energy dependence indicated by the measurements is at variance with the prediction (Figure 16).

CHAPTER VII

CONCLUSIONS

Absolute cross sections have been measured for the formation of excited hydrogen atoms in the 3s, 3p and 3d states by protons in targets of helium and nitrogen. The experimental technique required a quantitative measurement of the Balmer alpha photons emitted in spontaneous radiative decay by atoms in these states. The three parent states were separately identified by their different lifetimes. The measurements were made for impact energies ranging from 75 to 400 keV, a range in which approximations made in certain theoretical treatments are expected to be valid. In addition, absolute cross sections for the destruction of excited H atoms in the 3s state have been measured. Wherever possible the measurements have been compared with theoretical predictions and with other experimental work.

The cross sections for capture into 3s states are by far the largest of the three capture cross sections which were measured. Relative determinations have been made with an uncertainty of about ± 15 percent, but the possible error in absolute calibration may be as much as ± 50 percent. Within experimental error, there is agreement with other measurements[10] in the narrow interval where there is an overlap in the range of impact energies. In the case of a helium target, theoretical predictions[2] are available, and these appear to be at the upper limit of the estimated experimental error. The dependence on energy is in good agreement. The

cross section for a nitrogen target is roughly three times larger than for a target of helium.

The cross sections for capture into the 3d and 3p states are one to two orders of magnitude smaller than the 3s cross sections in the energy range of this experiment. Correspondingly, the uncertainties in measurements of these cross sections are much larger. However, there appears to be no serious disagreement with other experimental work.[10] In fact, the agreement appears surprisingly good. Theoretical predictions for the 3d capture cross section in helium are apparently in as good agreement as the 3s cross sections, although uncertainty in the measurements is too large to allow detailed comparison. The measured values of the cross section for capture into the 3p state from helium all lie below the theory by a factor of at least four. This discrepancy indicates a substantial error in the prediction of this cross section, and a suggestion is made for possible improvement of the theory by the inclusion of coupling to other states. For a nitrogen target, the fraction of the atoms formed in the p and d states is slightly larger than for helium.

Measured cross sections for destruction of excited H atoms in the 3s state are compared with theoretical predictions[1] of the cross section for ionization of these atoms. The theory indicates that under the conditions of this experiment, almost all inelastic collisions by H(3s) atoms result in ionization. There appear to have been no previous measurements of these cross sections. The uncertainty in the present measurements is large, ranging from ± 40 percent to ± 70 percent, and the energy dependences indicated by the measurements differ somewhat from those of the predictions. However, the agreement in magnitude is satisfactory since

most of the predicted values of the cross sections lie within the estimated experimental uncertainties. This cross section is several orders of magnitude larger than the cross section for capture into the 3s state.

Better measurements are needed for a more detailed comparison with theory, particularly in the case of the cross sections for capture into the 3d and 3p states. An alternative arrangement of the experimental apparatus is described to accomplish this purpose. In this regard, the possibility of accidental Stark mixing of the 3p and 3d states should receive further investigation. The cross section for the collisional excitation of ground state H atoms offers a new avenue for further research.

APPENDIX I

DEFINITION OF CROSS SECTION

A "cross section" as used in the present context is a measure of the probability that a certain event, process, or reaction will result from the collision of two microscopic particles. Cross sections are of two broad types: total and differential. A total cross section usually refers to the total probability of producing a certain species of collision product, whereas a differential cross section is further restricted, as its name implies, to the probability per unit interval of one or more continuous variables describing the given collision product, e.g., emission angle, kinetic energy, etc. The remarks which follow are pertinent to the concept of a total cross section. The value of a cross section will, of course, depend on the particular process being considered and on the nature of the two colliding particles. Although the concept of a cross section may be generalized to more complex cases, this discussion is restricted to collisions of two particles, but the particles are allowed to have internal structure which can be altered in the collision.

In observing the occurrence of processes on an atomic scale, it is inevitable that measurements be made not of a single collision between two particles whose collision parameters are well defined. The Heisenberg uncertainty principle prohibits such a measurement. Instead, an aggregation of particles of one type may be caused to interact with an

aggregation of the other type, and if measurements are made of the number of each type of colliding particle, their relative velocities, and the number of occurrences of the desired event, a probability of occurrence may be inferred in the form of a collision cross section.

There are several ways of developing a precise definition of a total collision cross section, but the derivation which follows is particularly pertinent to the present experiment. Suppose that particles of one type enter the collision region as a beam having a current of F particles per second. Let us call these particles the projectiles. For simplicity, let us assume that all the projectiles have the same velocity. (When the magnitude of the cross section being measured depends on the relative velocity of the colliding particles, the requirement of a monoenergetic beam of projectiles is not only a simplification but is necessary for meaningful measurements.) The second set of particles, which we term target particles, should also have a uniform velocity for the same reason.

Although the value of a total cross section is independent of the frame of reference to which it is referred, let us consider the interaction in the coordinate system at rest with respect to the target particles. (In the present experiment, this was the laboratory frame. Thermal velocities of the target particles were ignored since they were negligible in comparison to the projectile velocities.) In this reference frame, consider the probability dP of a collision of the type of interest within an infinitesimal volume element dxdydz oriented so that the x axis is parallel to the velocity of the projectiles. The probability of occurrence of such a collision is clearly proportional to

the target density ρ and to the size of the volume element

$$dP \propto \rho dxdydz \tag{53}$$

provided that the target is sufficiently tenuous that no target particle within dxdydz obscures to the projectiles another target within the volume element. If J is the current density at some point R within the volume element (particles per unit area per unit time), and if $N(x,y,z)$ is the number of events of the given type occurring per second per unit volume at R, then the number of events occurring within the volume element is proportional to J and to dP and is given by

$$N(x,y,z)\ dxdydz = Q\ J\ \rho dxdydz \tag{54}$$

where Q is introduced as a constant of proportionality. This constant has dimensions of area and is termed the cross section for the process.

If the collision process being considered were the classical scattering of hard spheres, the cross section Q would be πr^2 where r is the sum of the radii of the target and projectile spheres.

Equation (54) refers to an infinitesimal volume whereas measurements must, of course, be made for a finite volume. Let $N(x)$ be the number of events occurring per unit length along the x axis at x. Then since both J and ρ may be functions of position,

$$N(x)\ dx = dx \iint_{yz} N(x,y,z)\ dzdy = Qdx \iint_{yz} J(x,y,z)\ \rho(x,y,z)\ dzdy \tag{55}$$

For experiments such as the present one in which the target density is uniform throughout the interaction region, ρ may be taken outside the integral. Since J is related to $F(x)$, the beam current at x, by the equation

$$\iint_{yz} J(x,y,z)\, dzdy = F(x) \tag{56}$$

equation (55) reduces to

$$N(x)\, dx = Q\rho\, F(x)\, dx \tag{57}$$

In those cases where the target is sufficiently "thin" and the length d is sufficiently small that $F(x)$ is essentially unchanged between x and $x + d$, the number of events per second occurring between x and $x + d$ is

$$N(x)\, d = Q\rho\, F(x)\, d \tag{58}$$

This equation is frequently used as an operational definition of Q, the cross section, since the quantities Nd, ρ, F, and d are, in principle, measurable. However, one must be assured before using equation (58) that the assumptions made in its derivation are valid for the experiment to which it is applied. Because of beam neutralization, it became necessary to use equation (57) as the point of departure for the analysis of data from the present experiment.

It might also be worth noting that, in the present experiment, actual occurrences of the processes of interest, the direct capture of an electron into the 3s, 3p, and 3d states, were not detected at all

but were inferred from measurements of a consequent event, the emission of a Balmer alpha photon. The complexities of the experiment were due to the difficulties encountered in separating the contributions to the Balmer alpha emission from the three different parent levels and to the difficulties caused by other processes which either prevented the n=3 atoms from emitting or else created atoms in these states through other mechanisms than that of direct electron capture.

APPENDIX II

JUSTIFICATION OF THE NEGLECT OF THE EXCITATION OF GROUND STATE NEUTRAL ATOMS IN THE BEAM

There is a possibility that ground state neutral atoms which are formed in the beam can be excited into the n=3 level by a second collision. This process was neglected in the analysis of data because the experimental test described on page 35 indicated that the effect of this process on the measurements of Q_{3s} was negligible. The cross section for the excitation of neutral H atoms, $Q_{x,3\ell}$, has been neither predicted nor measured for targets of helium or nitrogen in the energy range of the present experiment. However, a useful indication of the importance of this process may be obtained by a consideration of available predictions for the excitation of neutral H atoms on a target of atomic H.

Consider the importance of $Q_{x,3\ell}$ in the coefficients of the first three exponentials of equation (20). For convenience we reproduce the coefficient of the 3s exponential as an example.

$$Q_{3s}\left\{\frac{\sigma_s}{\frac{1}{v\tau_{3s}}+\rho Q_i}+\frac{\sigma_c}{\frac{1}{v\tau_{3s}}+\rho Q_i-\rho(\sigma_s+\sigma_c)}\right\} \tag{59}$$

$$+Q_{x,3s}\left\{\sigma_c\left[\frac{1}{\frac{1}{v\tau_{3s}}+\rho Q_i}-\frac{1}{\frac{1}{v\tau_{3s}}+\rho Q_i-\rho(\sigma_s+\sigma_c)}\right]\right\}$$

For a target of helium at 10^{-3} Torr, the denominators of the fractions are dominated by $1/v\tau_{3S}$ in the energy range of the present experiment. The two fractions within the square bracket are therefore nearly equal and their difference is small in comparison to their sum. Furthermore, σ_c is less than σ_s for the energies of this experiment, ranging from 0.6 σ_s at 75 keV to 0.01 σ_s at 400 keV, so that the coefficient of $Q_{x,3s}$ ranges from 14 percent of the coefficient of Q_{3s} at 75 keV to about 0.1 percent at 400 keV. For a nitrogen target at 0.6 micron, the range is 14 percent to 0.2 percent.

There has been no publication of measurements or predictions of $Q_{x,3s}$ for targets of helium or nitrogen in the energy range of the present experiment. Hughes, et al.[66] have recently reported both $Q_{x,3s}$ and Q_{3s} for a nitrogen target for impact energies from 7.5 to 35 keV, a range which apparently includes the maxima of both cross sections. These measurements indicate that Q_{3s} is larger than $Q_{x,3s}$ by a factor which increases from 1.1 to four as the impact energy increases from 7.5 to 35 keV. Unfortunately, this observation is of limited value in assessing the ratio of these cross sections for impact energies between 75 and 400 keV, since Q_{3s} will undoubtedly decrease more rapidly than $Q_{x,3s}$ at large impact energies.

However, for a target of atomic hydrogen, the excitation cross section, $Q_{x,3s}$, has been calculated by Bates and Griffing[28] and the electron capture cross section Q_{3s} by Bates and Dalgarno[4] and independently by Jackson and Schiff.[3] It might be expected that the ratio of these cross sections in atomic hydrogen would be indicative of the value

of the same ratio for a target of helium or nitrogen. If the ratio $Q_{x,3s}/Q_{3s}$ is taken from these predictions, the second line of expression (59) is found to have a value between three and four percent of the first line, for all energies between 75 and 400 keV. A similar calculation made for the 3p states, again taking the ratio $Q_{x,3p}/Q_{3p}$ from the predictions by Bates and Griffing[28] and by Bates and Dalgarno[4] for a target of atomic hydrogen, shows that the term containing $Q_{x,3p}$ is 0.2 percent to one percent of the term in Q_{3p}. For the 3d state the $Q_{x,3d}$ term ranges from 0.5 to 10 percent of the Q_{3d} term.

By these arguments, equation (20) may now be reduced to the following, with the introduction of an error of at most a few percent in the values of the cross sections $Q_{3\ell}$:

$$G_\alpha(x) = \left\{\frac{1}{v(\sigma_s+\sigma_c)}\right\}\left\{\sum_{\ell=0}^{2} A_{3\ell\to 2\ell'}\left[\frac{\sigma_s Q_{3\ell}}{\frac{1}{v\tau_{3\ell}} + \rho Q_i}\right.\right. \tag{60}$$

$$\left.\left. + \frac{\sigma_c Q_{3\ell}}{\frac{1}{v\tau_{3\ell}} + \rho Q_i - \rho(\sigma_s+\sigma_c)}\right]\left[1 - e^{-\left(\frac{1}{v\tau_{3\ell}} + \rho Q_i\right) x}\right]\right.$$

$$\left. - \sigma_c\left[\sum_{\ell=0}^{2} A_{3\ell\to 2\ell'}\left(\frac{Q_{3\ell} - Q_{x,3\ell}}{\frac{1}{v\tau_{3\ell}} + \rho Q_i - \rho(\sigma_s+\sigma_c)}\right)\right]\right.$$

$$\left. \times\left[1 - e^{-\rho(\sigma_s+\sigma_c) x}\right]\right\} + K$$

The last exponential term in equations (20) and (60) has a decay

length $[\rho(\sigma_s+\sigma_c)]^{-1}$ strongly dependent on the target gas density. At pressures of the order of 10^{-3} Torr of helium or 6×10^{-4} Torr of nitrogen the ratio of this decay length to the decay length of the 3s state, $v\tau_{3s}$, is not sufficiently large to allow accurate separation of these terms by analysis of the data. At target gas pressures of the order of 10^{-4} Torr, this decay length is several times longer than the observation region, and again an accurate determination of the coefficient cannot be made from the data. At the lower energies in the range of this experiment, $Q_{3\ell}$ and $Q_{X,3\ell}$ may be of the same order of magnitude if a comparison of the predictions by Bates and Dalgarno[4] and by Bates and Griffing[28] for a target of atomic hydrogen is any indication. The difference $Q_{3\ell} - Q_{X,3\ell}$ may therefore tend to be small. At higher energies, where the difference in these two cross sections increases, σ_c is small. Also, the exponential factor, having a long decay length in comparison to the length of the observation region, will not exceed 0.26 for helium at 10^{-3} Torr, or 0.54 for nitrogen at 6×10^{-4} Torr (75 keV values -- smaller at higher energies). According to these predictions, then, the contribution to $G_\alpha(x)$ represented by this term is negligible.

APPENDIX III

Table 7. Absolute Cross Sections for the Formation and Destruction of Excited H Atoms in the 3s, 3p, and 3d States

Impact Energy (keV)	Cross Sections for Electron Capture by Protons into the 3s, 3p, and 3d States of H (units of 10^{-20} cm^2) Q_{3s}	Q_{3p}	Q_{3d}	Cross Section for Collisional Destruction of H atoms in the 3s State (units of 10^{-16} cm^2) Q_i
			Helium Target	
75	96.3	16.	1.2	3.52
100	59.5	1.7	1.2	2.62
125	33.8	0.41	0.82	2.18
150	17.4	1.3	0.30	1.16
200	6.73	0.42	0.10	0.500
250	3.65	0.19	0.074	0.238
300	1.91	0.18		0.123
350	0.958	0.079		0.069
			Nitrogen Target	
75	290	117	7.37	10.6
100	175	26.6	8.13	8.46
125	125	15.6	4.47	6.98
150	69.7	3.94	4.09	6.02
168	61.2	11.8	0.813	5.58
250	12.6	2.87	0.950	4.18
300	6.03	2.29	0.220	3.70
400	1.90			3.05

REFERENCES*

1. D. R. Bates and J. C. G. Walker, Planetary and Space Science, 14, 1367 (1966).

2. R. A. Mapleton, Phys. Rev. 122, 528 (1961).

3. J. David Jackson and Harry Schiff, Phys. Rev. 89, 359 (1953).

4. D. R. Bates and A. Dalgarno, Proc. Phys. Soc. (London) A66, 972 (1953).

5. D. R. Bates and A. Dalgarno, Proc. Phys. Soc. (London) A65, 919 (1952).

6. C. F. Barnett and H. K. Reynolds, Phys. Rev. 109, 355 (1958).

7. P. M. Stier and C. F. Barnett, Phys. Rev. 103, 896, (1956).

8. R. H. Hughes, H. R. Dawson, B. M. Doughty, D. B. Kay, and C. A. Stigers, Phys. Rev. 146, 53, (1966).

9. R. H. Hughes, B. M. Doughty and A. R. Filippelli, Phys. Rev. 173, 172 (1968).

10. R. H. Hughes, C. A. Stigers, B. M. Doughty, and E. D. Stokes, Phys. Rev. to be published May, 1970.

11. E. P. Andreev, V. A. Ankudinov, and S. V. Bobashev, Fifth International Conference on the Physics of Electronic and Atomic Collisions, Leningrad, U.S.S.R., July 17-23, 1967 (Nauka Publishing House, 1967) p. 307.

12. A. C. Riviere and D. R. Sweetman, Proceedings of the Sixth International Conference on Ionization Phenomena in Gases (SERMA, Paris, 1963) Vol. 1, p. 105.

13. A. C. Riviere and D. R. Sweetman, Proceedings of the Third International Conference on the Physics of Electronic and Atomic Collisions, London, 1963 (North Holland Publishing Co., Amsterdam, 1964) p. 734.

14. R. LeDoucen and J. Guidini, Sixth International Conference on the Physics of Electronic and Atomic Collisions, Cambridge, Massachusetts, (M.I.T. Press, Cambridge, 1969) p. 454.

*Abbreviations used herein conform to those found in the American Institute of Physics Style Manual, 1967.

15. A. H. Futch and K. G. Moses, Fifth International Conference on the Physics of Electronic and Atomic Collisions, Leningrad, U.S.S.R., July 17-23, 1967, (Nauka Publishing House, Leningrad, 1967), p. 12.

16. R. H. MacFarland and A. H. Futch, Jr., Sixth International Conference on the Physics of Electronic and Atomic Collisions, Cambridge, Massachusetts, July 28-August 2, 1969, (MIT Press, Cambridge, 1969), p. 441.

17. A. H. Futch and C. C. Damm, Nuclear Fusion 3, 124 (1963).

18. R. A. Mapleton, Phys. Rev. 130, 1839 (1963).

19. B. H. Bransden and L. T. Sin Fai Lam, Proc. Phys. Soc. (London) 87, 653 (1966).

20. C. C. Damm, J. H. Foote, A. H. Futch, and R. F. Post, Phys. Rev. Letters 10, 323 (1963).

21. D. R. Sweetman, Nuclear Fusion Supplement 1, 279 (1962).

22. W. L. Wiese, M. W. Smith, and B. M. Glennon, Atomic Transition Probabilities, Volume I Hydrogen Through Neon, National Bureau of Standards, U.S. Department of Commerce, Distributed by: Superintendent of Documents, U. S. Government Printing Office, Washington, D. C. 20402, AD 634145.

23. J. L. Edwards and E. W. Thomas, Phys. Rev., 165, 16 (1968).

24. H. A. Bethe and E. E. Salpeter, Quantum Mechanics of One-and Two-Electron Atoms, (Academic Press, Inc., New York, 1957).

25. R. H. Hughes, H. R. Dawson and B. M. Doughty, J. Opt. Soc. Am., 56, 830 (1966).

26. A. S. Goodman and D. J. Donahue, Phys. Rev. 141, 1, (1966).

27. V. A. Ankudinov, S. V. Bobashev, and E. P. Andreev, Sov. Phys. - JETP, 21, 26 (1965).

28. D. R. Bates and G. Griffing, Proc. Phys. Soc. (London), A66, 961 (1953).

29. J. R. Oppenheimer, Phys. Rev. 31, 349, 1928.

30. R. M. May, Nuclear Fusion, 4, 207, (1964).

31. R. H. Hughes, H. R. Dawson, and B. M. Doughty, Phys. Rev. 164, 166 (1967).

32. H. Ishii and K. I. Nakayama, Transactions of the Eighth National Vacuum Symposium and Second International Congress, (Pergamon Press, Oxford 1962) p. 519.

33. T. Takaishi, Trans. Faraday Soc., 61, 840 (1965).

34. Saul Dushman, Scientific Foundations of Vacuum Technique, (John Wiley and Sons, New York, 1962) Second edition pp. 58-59.

35. I. C. Percival and M. J. Seaton, Phil. Trans. Roy, Soc. London, A251, 113 (1958).

36. I. C. Percival, private communication.

37. Yardley Beers, Introduction to the Theory of Error, (Addison-Wesley Publishing Co., Cambridge, Mass., 1953).

38. J. R. Hiskes, Phys. Rev. 180, 146, (1969).

39. J. R. Hiskes, Lawrence Radiation Laboratory, Livermore, California, Report UCRL-50602, unpublished.

40. J. R. Hiskes, private communication.

41. S. T. Butler and R. M. May, Phys. Rev. 137, A10, (1965).

42. L. T. Sin Fai Lam, Proc. Phys. Soc., (London), 92, 67, (1967).

43. R. A. Mapleton, Phys. Rev. 126, 1477 (1962).

44. K. H. Berkner, W. S. Cooper III, S. N. Kaplan, and R. V. Pyle, Phys. Rev. 182, 103, (1969).

45. E. W. Thomas, G. D. Bent, and J. L. Edwards, Phys. Rev., 165, 32, (1968).

46. E. W. Thomas and G. D. Bent, Phys. Rev., 164, 143 (1967).

47. J. G. Lodge, Proc. Phys. Soc. (London), Series 2, B2, 322 (1969).

48. D. A. Dahlberg, D. K. Anderson, and I. E. Dayton, Phys. Rev. 164, 20, (1967).

49. L. Colli, F. Cristofori, G. E. Frigerio, P. G. Sona, Phys. Letters 3, 62, (1962).

50. D. Jaecks, B. Van Zyl, R. Geballe, Phys. Rev. 137, A340, (1965).

51. V. Dose, Helv. Phys. Acta 39, 683, (1966).

52. E. P. Andreev, V. A. Ankudinov, and S. V. Bobashev., Sov. Phys. - JETP 23, 375, (1966).

53. G. Ryding, A. B. Wittkower, H. B. Gilbody, Proc. Phys. Soc. (London) 89, 547, (1966).

54. F. J. DeHeer, J. Van Eck, and J. Kistemaker, Proceedings of the Sixth International Conference on Ionization Phenomena in Gases (SERMA, Paris, 1963), Vol. I, p. 73.

55. D. Pretzer, B. Van Zyl, R. Geballe, Proceedings of the Third International Conference on the Physics of Electronic and Atomic Collisions, London, 1963 (North Holland Publishing Co., Amsterdam, 1964) p. 618.

56. T. D. Gaily, D. H. Jaecks, R. Geballe, Phys. Rev. 167, 81, (1968).

57. E. P. Andreev, V. A. Ankudinov, S. V. Bobashev, V. B. Matveev, Sov. Phys. - JETP, 25, 232, (1967).

58. J. E. Bayfield, Phys. Rev. 182, 115, (1969).

59. P. J. O. Teubner, W. E. Kauppila, W. L. Fite, R. J. Girnius, Proceedings of the Sixth International Conference on the Physics of Electronic and Atomic Collisions, Cambridge, Massachusetts, (M.I.T. Press, Cambridge, 1969), p. 109.

60. I. A. Sellin, Phys. Rev. 136, A1245, (1964).

61. E. P. Andreev, V. A. Ankudinov, and S. V. Bobashev, Proceedings of the Fifth International Conference on the Physics of Electronic and Atomic Collisions, Leningrad, U.S.S.R., July 17-23, 1967, (Nauka Publishing House, Leningrad, 1967), p.309.

62. I. A. Sellin and L. Granoff, Phys. Letters 25A, 484, (1967).

63. B. L. Donnally, T. Clapp, W. Sawyer, M. Schultz, Phys. Rev. Letters 12, 502, (1964).

64. A. Cesati, F. Cristofori, L. M. Colli, P. G. Sona, Energia Nucleare 13, 649, (1966).

65. D. A. Dahlberg, D. K. Anderson, and I. E. Dayton, Phys. Rev. 170, 127, (1968).

66. R. H. Hughes, A. R. Filippelli and H. M. Petefish, Phys. Rev., 3rd Series A1, 21 (1970).

VITA

Lee Edwards was born on May 11, 1935 to Mr. and Mrs. Joseph Lee Edwards of Atlanta, Georgia. He attended the Lovett School and in June, 1953, was graduated from Northside High School of Atlanta as valedictorian of his class. In June, 1957, he received from the Georgia Institute of Technology the degree of Bachelor of Science in physics with highest honor.

During the two years of his service in the United States Navy, he was engaged in low temperature research. He was employed as a graduate laboratory assistant in the Physics Department of the Carnegie Institute of Technology while pursuing graduate studies. He was graduated in June, 1961, with the degree of Master of Science in physics.

He was employed as manager of the Industrial Division of Kelvin and Hughes America Corporation of Annapolis, Maryland, until 1964 when he joined the Engineering Experiment Station of the Georgia Institute of Technology as a Research Physicist. He resumed graduate study in the School of Physics at that time. In 1965, with the aid of a traineeship from the National Aeronautics and Space Administration he was granted a leave of absence from the Experiment Station to devote full time to these studies.